


RESEARCH

Open Access



# Polydatin nanoparticles attenuate oxidative stress and histopathological changes in streptozotocin model of diabetic nephropathy: targeting Nrf2/HO-1/NF- $\kappa$ $\beta$ signaling pathways

Manal Abdul-Hamid<sup>1\*</sup> , Sanaa R. Galaly<sup>1</sup>, Hanaa M. Mohamed<sup>2</sup>, Fatma Mostafa<sup>1</sup> and Adel Abdel-Moneim<sup>3</sup>

## Abstract

**Background** One of the most prevalent and serious side effects of diabetes mellitus is diabetic nephropathy, which is characterized by abnormalities in kidney structure that can occur before kidney function declines. Up to 90% of persons with diabetic nephropathy and 40% of adults with severe diabetic nephropathy are unaware that they have kidney disease. Through Nrf2/HO-1/NF  $\kappa$  $\beta$ /TNF  $\alpha$  signaling pathways, biochemical, oxidative stress, and antioxidant biomarkers, ultrastructural, immunohistochemical, and histopathological studies, so we attempt to evaluate the potential corrective mechanisms of polydatin nanoparticles against diabetic nephropathy in comparison with polydatin and metformin.

**Results** POLY-CSNPs, POLY, and METF treatment lowered fasting superoxide dismutase, catalase activities, and glutathione content in treating the diabetic blood sugar level, glycosylated hemoglobin percentage, and oxidative stress such as lipid peroxidation level, and also enhanced antioxidant biomarkers like superoxide peroxidase, superoxide dismutase, catalase activities, and glutathione content in treating the diabetic nephropathy. POLY-CSNPs, POLY, and METF also significantly reduced the area % of immunohistochemical reaction of TNF  $\alpha$  (tumor necrosis factor alpha) and NF  $\kappa$  $\beta$  (nuclear factor-kappa- $\beta$ ), while significantly increasing the mRNA expression's levels for nuclear factor erythroid 2-related factor 2 and heme oxygenase-1. The results observed that POLY-CSNPs showed extremely significant efficacy in treated diabetic rats as contrasted with POLY. Histological and ultrastructural studies showed marked improvement in glomeruli, basal laminae, and proximal tubules appearing nearly identical to the normal.

**Conclusions** POLY-CSNPs revealed a marked ameliorative effect on diabetic nephropathy via its anti-inflammatory, antioxidant, and prolonged-release properties.

**Keywords** Diabetic nephropathy, Metformin, Polydatin nanoparticles, Oxidative stress biomarkers, Histopathology, Ultrastructure

\*Correspondence:

Manal Abdul-Hamid

medo\_bio@yahoo.com; manal.mohamed3@science.bsu.edu.eg

Full list of author information is available at the end of the article



© The Author(s) 2023. **Open Access** This article is licensed under a Creative Commons Attribution 4.0 International License, which permits use, sharing, adaptation, distribution and reproduction in any medium or format, as long as you give appropriate credit to the original author(s) and the source, provide a link to the Creative Commons licence, and indicate if changes were made. The images or other third party material in this article are included in the article's Creative Commons licence, unless indicated otherwise in a credit line to the material. If material is not included in the article's Creative Commons licence and your intended use is not permitted by statutory regulation or exceeds the permitted use, you will need to obtain permission directly from the copyright holder. To view a copy of this licence, visit <http://creativecommons.org/licenses/by/4.0/>.

## 1 Background

One of the diabetic problems is DN (diabetic nephropathy) which is known as diabetic kidney illness [1, 2]. Diabetic nephropathy affects 40% of people who have type 2 diabetes mellitus [3, 4]. DN leads to glomerular and tubular damage and the onset of kidney disease [2]. Albumin exposure is increased in tubular cells and causes cytotoxicity within the proximal and distal tubule cells via enhancing a variety of pathways of intracellular signaling [5] that trigger the inflammatory, vasoactive [6], and fibrotic substances release [7], resulting in interstitial injury and eventually going to permanent loss of kidney function [8]. Furthermore, albumin exposure that is increased in tubular cells can induce the apoptosis of the cells, resulting in decreased nephron functionality [8, 9].

The aggregation of macrophages in DN is caused by the pathways of NF  $\kappa$ B activation by TNF  $\alpha$  and other cytokines [10]. Increased advanced glycation end products (AGEs) and reactive oxygen species (ROS) stimulate leukocytes in diabetic patients, causing them to discharge proteases and superoxide radicals in the kidney [11]. TNF causes the formation of ROS in the kidney cells regardless of the hemodynamic pathways, and glomerular capillary wall modification, and as a result, enhances urinary albumin excretion [12]. In histological studies, DN showed irregular glomeruli as well as necrosis and congestion of the nephron's distal and proximal tubules and thickening of the Bowman's capsule [13, 14]. Ultrastructural examinations also revealed a glomerular basement membrane thickness enveloped with podocytes and an abnormal nuclear membrane, a large subpodocytic space, and numerous vacuoles in the cytoplasm. The nucleus of the proximal convoluted tubule was also elongated, the basal mitochondria were disorganized [15], and the imbalance between oxidative stress and antioxidant elements causes both of these pathways [16].

Free radicals and ROS are scavenged by antioxidants [17]. Polydatin (POLY) is a glycoside of resveratrol and a major active element of a Chinese traditional medicine plant called *Polygonum cuspidatum* (*Polygonaceae*) [18]. POLY has antioxidant properties that can aid in body protection from diabetic complications and oxidative stress [19, 20]. It also modulates glucose and lipid metabolism to reduce diabetes [21]. POLY protects DN rats from renal inflammation by lowering the levels of inflammatory factors in the kidney tissue, which has an anti-inflammatory protective effect [22]. POLY improved hyperglycemia, decreased inflammatory cells, and improved glomerular and tubular structures in diabetic rats [23]. The therapeutic applications of POLY are limited despite its promising pharmacological

characteristics because of its poor water solubility, chemical instability in aqueous alkaline media, and significant first-pass metabolism [24]. Nanoparticles can serve as various delivery systems—pharmaceutical carriers due to their small size and huge surface area [25]. Therefore, we investigate the potential beneficial effects of n-CSNPs against diabetic nephropathy [26], since the polydatin nanoparticles are biocompatible and more potent at preventing diabetes than free polydatin [27]. The American Diabetes Association (ADA) suggests metformin, a synthetic biguanide derivative that is frequently used to treat T2DM, as first-line therapy [28, 29]. Metformin successfully treated metabolism disorders of glycolipid, kidney function harm, and oxidative stress in rats with diabetes [30]. This research tries to assess the potential corrective mechanisms of polydatin nanoparticles against diabetic nephropathy compared to polydatin and metformin. So, this study was achieved through measurements of Nrf2/HO-1/NF  $\kappa$ B/TNF  $\alpha$  signaling pathways, biochemical, oxidative stress, antioxidant biomarkers, ultrastructural, immunohistochemical and histopathological studies.

## 2 Materials and methods

### 2.1 Reagents and chemicals

The powders of nicotinamide (NA), STZ (streptozotocin), and polydatin (POLY) were obtained from Sigma-Aldrich Co. MO, USA. The tablets of METF (Glucophage Xr 1000 mg) were obtained from Merck KGaA, Darmstadt, Germany. Chitosan with medium molecular weight of 200 kDa on average was obtained from Techno Pharmchem Co., Delhi, India.

### 2.2 Preparation of polydatin-loaded chitosan nanoparticles

Chitosan (CS) was dissolved in 2% glacial acetic acid (v/v) to create a chitosan solution (0.3%, w/v), which was then pH-adjusted to 4.8 with a 2% aqueous solution of NaOH. Chitosan solution (CS: POLY 3:1, w/w) was mixed with POLY solution dropwise for 30 min at 1000 rpm while being magnetically stirred. Then, the POLY/CS combination was gently and gradually mixed with an aqueous solution of tripolyphosphate (TPP) (CS: TPP 3:1, w/w), with steady stirring for one hour at 1500 rpm. Tween 80 (0.5%, w/v) was added to the mixture for coating after which it was continuously stirred for 30 min and sonicated for 15 min with a probe sonicator. Using a cooling centrifuge, the resulting nanoparticle suspension was centrifuged for 45 min at 14,000 rpm and 4 °C. The pellets were then dissolved in distilled water, lyophilized for 48 h in a freeze dryer, and kept in powder form at 4 °C [27, 31].

### 2.3 Induction of diabetes

Fifteen minutes after the intraperitoneal (i.p.) nicotinamide administration (110 mg/kg; formed in normal physiological saline), a streptozotocin single i.p. injection (50 mg/kg; soluble in 0.1 M cold citrate buffer with pH 4.5) induced experimental T2DM in overnight fasted rats [32], followed by an oral glucose load 10% after four hours to avoid hypoglycemia. After a week of NA/STZ injections, a sample of blood was drawn via the lateral tail vein, and fasting blood sugar level (FBS) was tested utilizing a glucometer (CERA-CHECK™ 1070, Korea). The experiment used stable diabetic rats whose levels of blood glucose were about 200 mg/dl.

### 2.4 Animal model

We used 48 male Wistar albino rats from the breeding unit of the Egyptian Organization for Biological Vaccine Production, Cairo, Egypt (VACSERA), weighing 100–135 g. Rats were given full diet pellets and free access to water. To rule out any intercurrent infections, we observed the animals for two weeks before the experiment started. In this report, we adopted the IACUC (Institutional Animal Care and Use Committee) guidelines and Approval (BS-FS-2018-14) by the National Rules for Animal Care that follow the Health National Institutes for the Laboratory Animals Care and Use (NIH Publication no. 8023, revised 1978). Six rats groups were formed, each containing eight rats. The rats were given all doses daily through gastric intubation for 30 days after STZ/NA administration for seven days. The first group (C) received 1% carboxymethyl cellulose (CMC) and acted as normal control animals. The second group (D) was given CMC 1% and acted as untreated diabetic control animals. The diabetic rats within the third group (D+CSNPs) got 50 mg/kg equivalent blank chitosan nanoparticles, soluble in CMC (1%) [27]. (D+POLY-CSNPs) was the fourth group consisting of diabetics who were given POLY-CSNPs containing 50 mg/kg POLY, soluble in CMC (1%) [27]. The fifth group acted as 50 mg/kg POLY-treated diabetics (D+POLY), soluble in CMC (1%) [27]. The sixth group (D+METF) received 100 mg/kg METF-treated diabetics, soluble in CMC (1%) [27].

### 2.5 Measuring of glucose

Fasting blood glucose (FBS) levels before treatment and after treatment with POLY-CSNPs, POLY, and METF were estimated in the samples of blood obtained from

the rat's lateral vein of the tail before killing with a glucometer with a 600 mg/dl maximum measuring power (CERA-CHECK™ 1070, Korea). Following kill, some collected blood samples were used to calculate blood glycosylated hemoglobin % (HbA1c%) by Biosystems (Spain) reagent kits.

### 2.6 Renal function assessment

Following kill, additional samples of blood were centrifuged for 20 min at around 560 g after being permitted to clot for two hours at the temperature of the room. The serum (clear supernatant) was easily extracted and kept at  $-20^{\circ}\text{C}$  before it was used to determine serum biochemical parameters for the kidney using an in vitro quantitative reagent kit purchased from Vitro Scient (Hannover, Germany) following the enzymatic, colorimetric method (urease) adjusted Berthelot reaction [33] to estimate urea level. Also, serum was used to determine serum uric acid using the enzymatic, colorimetric method (Uricase/PAP) with uricase and 4-aminoantipyrine [34] by an in vitro quantitative reagent kit procured from Vitro Scient (Hannover, Germany), and to determine creatinine by an in vitro quantitative reagent kit purchased from BioMed (Hannover, Germany) [35].

### 2.7 Oxidative stress and antioxidant biomarkers

Frozen kidneys were measured, cut, and homogenized in distilled water after being thawed and dissected. Oxidative stress and antioxidant biomarkers were determined using a clear supernatant of kidney homogenate. The MDA (lipid peroxidation) was calculated using the approach of Preuss et al. based on the conclusion that the level of malondialdehyde produced when polyunsaturated fatty acids break down [36]. In addition, the level of superoxide dismutase activity (SOD antioxidant enzyme) was calculated as per the Marklund and Marklund approach due to the pyrogallol inhibition auto-oxidation by catalyzing the breakdown of superoxide [37]. The level of antioxidant enzyme of CAT (catalase activity) was determined using the approach of Cohen et al. based on observing the potassium permanganate-catalyzed hydrogen peroxide enzyme breakdown [38]. The level of antioxidant enzyme of peroxidase activity (POX) was calculated as per the method of Kar and Mishra based on utilizing a pyrogallol as a substrate while  $\text{H}_2\text{O}_2$  is present [39]. The level of antioxidant enzyme of GSH (reduced glutathione concentration) was calculated using the approach of Beutler et al. based on the redox reaction, whereas GSH has a reducing power [40].

## 2.8 Real-time quantitative PCR

The effects of POLY-CSNPs, POLY, and METF on HO-1 and Nrf2 mRNA abundance were looked into using the reaction of the polymerase chain with quantitative reverse transcriptase (qRT-PCR). Isolation kits of total RNA were used to isolate total RNA from frozen kidney samples determined at 260 nm using cDNAs, made from two mg RNA and increased by applying SYBR green master mix (Thermo Scientific, USA) and the sets of primer {HO-1 primers (Forward: 5'-TGCTCAACATCCAGC TCTTTGA-3', Reverse: 5'-GCAGAATCTTGCACT TTGTTGCT-3'); Nrf2 primers (Forward: 5'-ATCCAG ACAGACACCAGTGGATC-3', Reverse: 5'-GGCAGT GAAGACTGAACTTTCA-3') and  $\beta$ -actin primers (Forward: 5'-TGTTTGAGACCTTCAACACC-3', Reverse: 5'-CGCTCATTGCCGATAGTGAT-3')}. The amplification data were evaluated by using the  $2^{-\Delta\Delta C_t}$  approach [41], and  $\beta$ -actin was used to normalize the data that displayed as control percent.

## 2.9 Histological and immunohistochemical studies

For histological studies, samples of the kidney were preserved in neutral formalin buffered (10%) for 24 h; after that, they were dehydrated using ethyl alcohol (ascending grades), cleared with xylene then submerged in paraffin, and inserted at 60 °C in paraffin wax. Hematoxylin and eosin [42] and Masson's trichrome staining [43] are used to dye parts with a thickness of 4–5  $\mu$ m.

## 2.10 Immunohistochemical and Histomorphometric studies

Immunohistochemical studies of NF  $\kappa$ B and TNF  $\alpha$  stains were used within other sections. For the avoidance of arbitrary binding, the sections were incubated in 3% H<sub>2</sub>O<sub>2</sub> to be blocked, then boiled in the buffer of

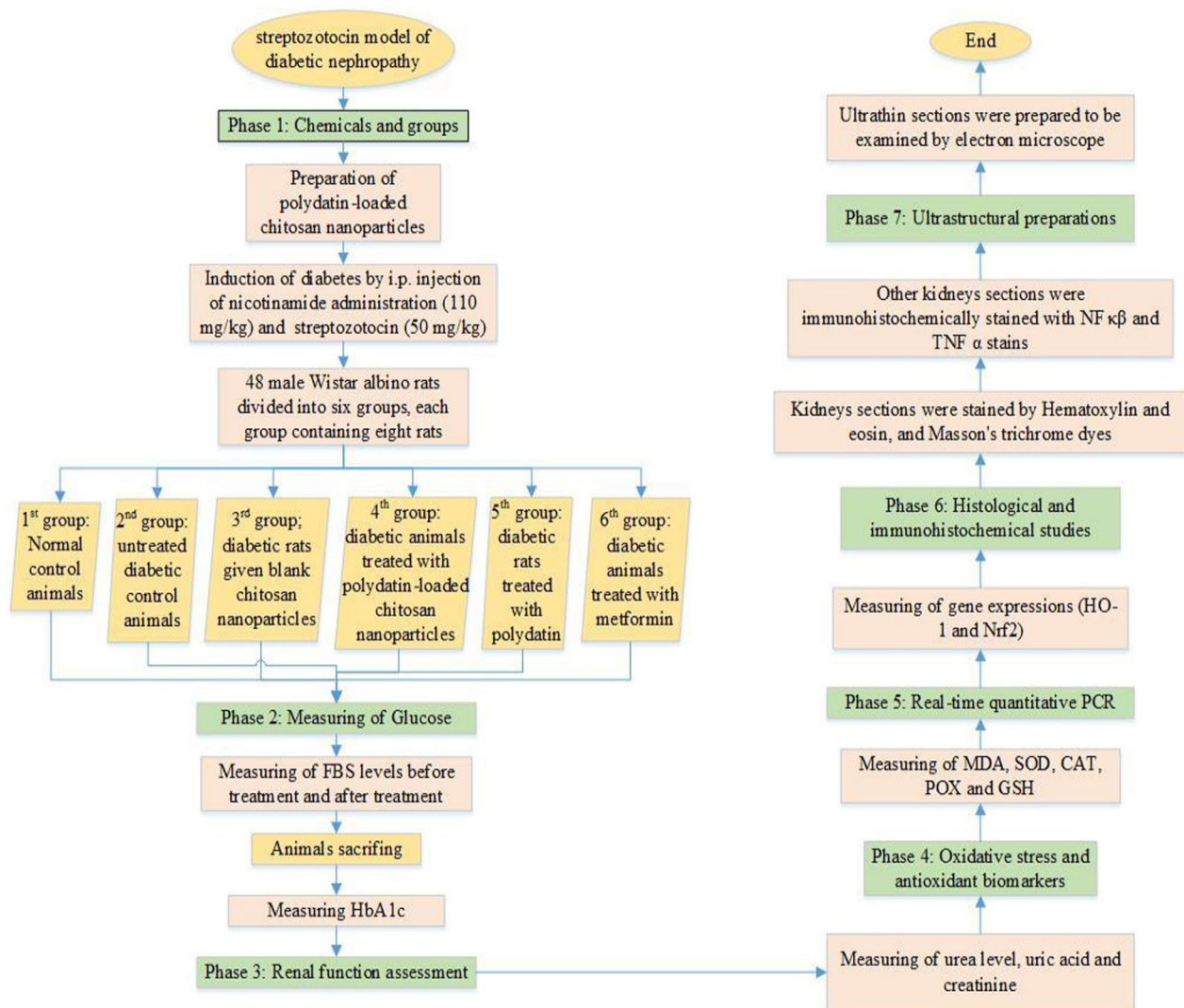
citrate (pH 6.0), and blocked by a block of protein. After that, the sections were examined using TNF  $\alpha$  and NF  $\kappa$ B-specific antibodies, then rinsed in a buffer solution of phosphate (PB), and incubated using the secondary antibody. Sections were washed and counterstained together with Mayer's hematoxylin; after that, sections were studied. Using the ImageJ software (Cambridge, England-based Leica Qwin 500 image system), histomorphometric analysis was completed to assess the mean area % of NF  $\kappa$ B and TNF  $\alpha$ . The mean area percentage (%) was evaluated from 10 randomly selected fields with no overlap and a 400 overall magnification for each rat [44].

## 2.11 Ultrastructural preparations

For ultrastructural studies, about 1 mm<sup>3</sup> of tissue of the kidney was cut and fixed in the solution of glutaraldehyde–formaldehyde (3%). Following a wash in PB (pH 7.4), these specimens were post-fixed in 1 % isotonic osmium tetroxide post for 1 h at 4 °C. Preparing sections for electron microscopic examination method were as follows [45]. To identify the desired location, we stained the semi-thin sections with toluidine blue. After that, we prepared ultrathin sections by using knives of ultramicrotome glass. We used lead citrate and uranyl acetate to dye the specimens; then, we used electron microscope transmission (Joel CX 100) to examine the specimens.

## 2.12 Statistical analysis

Data were analyzed, and findings were presented as mean  $\pm$  standard error. IBM SPSS Statistics 20 statistical software (IBM Corporation, NY, USA) was employed to examine the data. One-way analysis of variance (ANOVA) was employed to examine the results. Variances were shown as important at  $P < 0.05$ .



### 3 Results

#### 3.1 Body and kidney weights

The diabetic rats body weight revealed a significant ( $P < 0.001$ ) reduce in the weight relative to the normal control group, whereas after treatment with each of POLY-CSNPs, POLY, and METF, this decrease was significantly improved as opposed to the diabetic control group (Fig. 1a). According to what we had found, the kidney weight in the diabetic group displayed a significant rise in comparison with the control group, whereas it was markedly improved after treating with POLY-CSNPs, POLY, or METF relative to the animals of the diabetic group (Fig. 1b).

#### 3.2 Levels of fasting blood sugar and HbA1c%

In diabetic rats, FBS levels and HbA1c% observed significant ( $P < 0.001$ ) elevation in comparison with normal control rats, whereas blood glucose levels were significantly reduced in diabetic rats that had received each of POLY-CSNPs, POLY, and METF in contrast to the rats of the diabetic control group and rats of diabetic groups before treatment. In addition, diabetic rats treated with POLY-CSNPs revealed a highly significant ( $P < 0.001$ ) effect in HbA1c% relative to diabetic rats that had received POLY and METF ( $P < 0.05$ ) (Fig. 1c, d).

#### 3.3 Kidney function profile

In diabetic rats' serum, urea, creatinine, and uric acid levels were elevated significantly ( $P < 0.001$ ) in contrast to

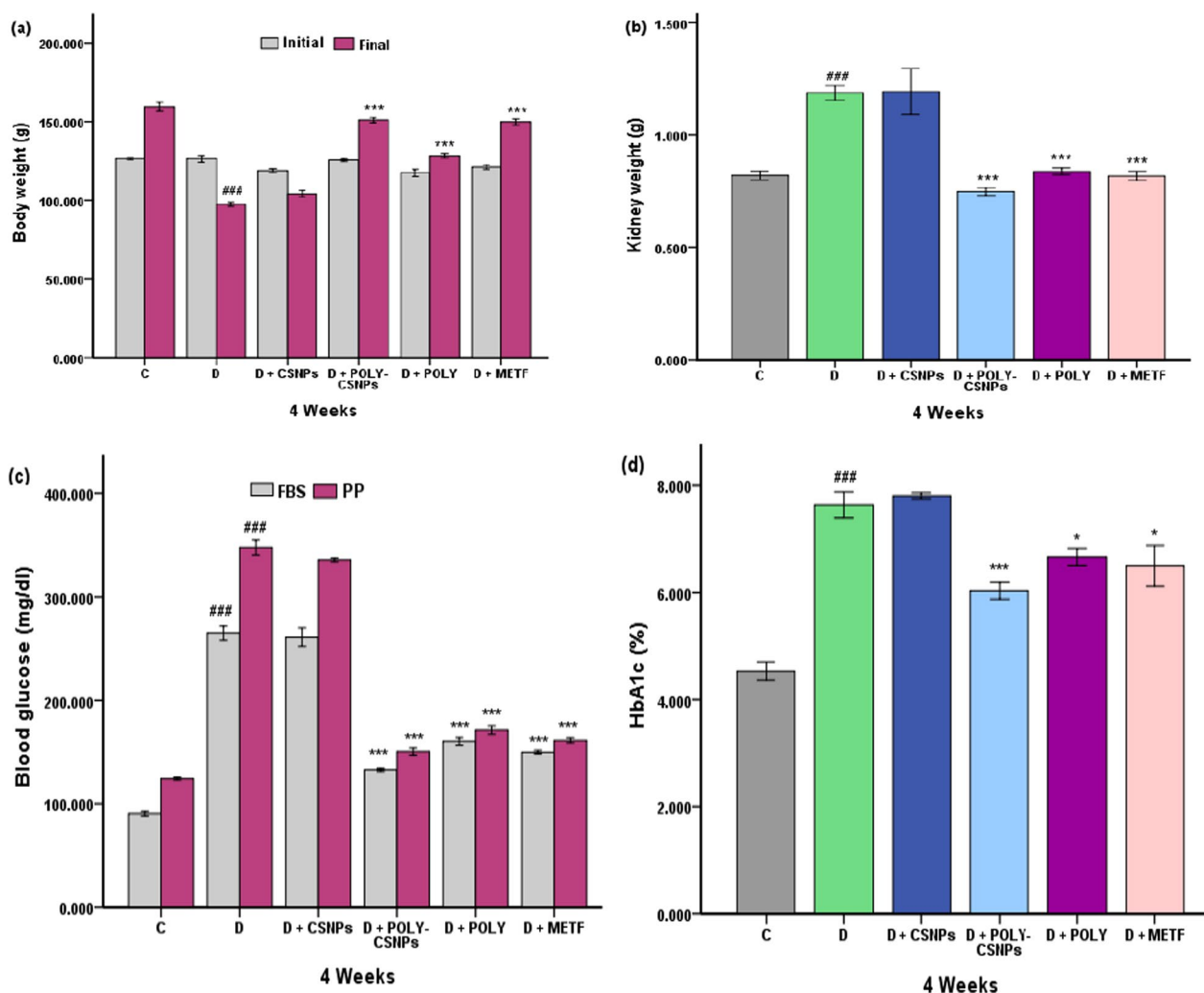


**Fig. 1 a–d** Body weight changes (g) between (initial body weight and final body weight), kidney weight (g), FBS prior treatment and FBS after treatment (mg/dl) and HbA1c (%) of normal control animals (C), diabetic control group (D), diabetic animals treated with blank chitosan nanoparticles (D + CSNPs), diabetic group treated with polydatin-loaded chitosan nanoparticles (D + POLY-CSNPs), polydatin (D + POLY), and metformin HCl (D + METF), respectively, for 4 weeks. Data are expressed as mean ± SEM (n = 6). <sup>###</sup>P < 0.001 versus control; <sup>\*</sup>P < 0.05; <sup>\*\*</sup>P < 0.01 and <sup>\*\*\*</sup>P < 0.001 versus diabetic control

the normal control rats, whereas oral administration of POLY-CSNPs, POLY, and METF to diabetic rats avoided the elevation in these levels compared to the rats of diabetic control (Table 1).

### 3.4 Kidney antioxidant and oxidative stress biomarkers

In animals with diabetes, the kidney displayed a noticeable ( $P < 0.001$ ) rise in MDA products; however, this change was significantly improved in diabetic rats that had received POLY-CSNPs more than in diabetic rats given each of POLY and METF when opposed to the rats of a diabetic control group. Concerning this study, antioxidant biomarkers such as SOD, POX, CAT activities, and GSH content displayed a significant ( $P < 0.001$ )

reduction in animals with diabetes when opposed to the rats of a normal control group. Diabetic rats treated with POLY-CSNPs and METF revealed a very significant amelioration effect ( $P < 0.001$ ) than rats treated with POLY in MDA content and POX activity ( $P < 0.01$ ), and GSH content and SOD activity ( $P < 0.05$ ) compared to diabetic control rats (Table 1).

### 3.5 Real-time PCR

HO-1 and Nrf2 gene expressions in kidney tissue were significantly ( $P < 0.001$ ) reduced in diabetic rats compared to the rats of normal control animals. There was no ameliorative change in diabetic animals that had received CSNPs, whereas diabetic rats that had received

**Table 1** Effect of POLY-CSNPs, POLY, and METF on urea, creatinine, uric acid, MDA, GSH, SOD, POX, CAT, Nrf2, and HO-1 in the studied groups

Tests	Groups					
	C	D	D+CSNPs	D+POLY-CSNPs	D+POLY	D+METF
Urea (mg/dl)	31.730±4.006	64.366±2.501 <sup>###</sup>	61.785±0.825	26.092±1.259 <sup>***</sup>	34.633±0.661 <sup>***</sup>	28.735±0.228 <sup>***</sup>
Creatinine (mg/dl)	1.857±0.163	3.692±0.246 <sup>###</sup>	3.618±0.312	1.876±0.087 <sup>***</sup>	2.025±0.062 <sup>***</sup>	1.975±0.136 <sup>***</sup>
Uric acid (mg/dl)	2.889±0.048	4.320±0.044 <sup>###</sup>	4.523±0.102	2.699±0.114 <sup>***</sup>	2.924±0.094 <sup>***</sup>	2.889±0.123 <sup>***</sup>
MDA (nmol/g protein)	208.667±34.296	452.539±19.257 <sup>###</sup>	485.560±24.157	246.695±34.996 <sup>***</sup>	314.156±15.748*	275.290±24.526 <sup>**</sup>
GSH (nmol/mg protein)	13.060±0.685	6.562±0.174 <sup>###</sup>	6.739±0.458	13.170±0.779 <sup>***</sup>	10.926±0.501 <sup>**</sup>	12.141±1.447 <sup>***</sup>
SOD activity (U/g protein)	1.194±0.094	0.643±0.041 <sup>###</sup>	0.645±0.051	1.179±0.080 <sup>***</sup>	1.026±0.061 <sup>**</sup>	1.130±0.045 <sup>***</sup>
POX activity (U/g protein)	1.084±0.048	0.571±0.055 <sup>###</sup>	0.586±0.055	1.059±0.126 <sup>***</sup>	0.908±0.026*	0.924±0.017 <sup>**</sup>
Catalase activity (U/g protein)	0.576±0.056	0.130±0.041 <sup>###</sup>	0.175±0.031	0.647±0.064 <sup>***</sup>	0.551±0.057 <sup>***</sup>	0.573±0.036 <sup>***</sup>
Nrf2 (Relative to control)	1.010±0.004	0.353±0.014 <sup>###</sup>	0.303±0.021	0.827±0.037 <sup>***</sup>	0.600±0.027 <sup>**</sup>	0.748±0.018 <sup>***</sup>
HO-1 (Relative to control)	1.510±0.153	0.520±0.042 <sup>###</sup>	0.587±0.018	1.057±0.046 <sup>***</sup>	0.823±0.015*	0.917±0.031 <sup>**</sup>

Data are expressed as mean ± SEM (n = 6). C: control rats; D: diabetic rats; D + CSNPs: diabetic rats treated with blank chitosan nanoparticles; D + POLY-CSNPs: diabetic rats treated with polydatin-loaded chitosan nanoparticles; D + POLY: diabetic rats treated with polydatin; D + METF: diabetic rats treated with metformin HCl; MDA: lipid peroxidation; GSH: reduced glutathione concentration; SOD: superoxide dismutase activity; POX: peroxidase activity; CAT: catalase activity; Nrf2: nuclear factor erythroid 2-related factor 2; HO-1: heme oxygenase-1. <sup>###</sup>*P* < 0.001 versus control; \**P* < 0.05, \*\**P* < 0.01 and \*\*\**P* < 0.001 versus diabetic control

POLY-CSNPs, POLY, and METF for 30 days displayed a significant improvement in HO-1 and Nrf2 genes expression levels (Table 1; Additional file 1: Fig. S1). Nrf2/HO-1 signaling pathway modulation resulted in POLY-CSNPs, POLY, and METF ameliorative role in the kidney of diabetic animals against apoptosis and kidney injury induced by oxidative stress, whereas POLY-CSNPs showed a significant amelioration in HO-1 and Nrf2 genes expression levels when compared to POLY (Additional file 1: Table S1).

### 3.6 Histological examination

Control animals' renal cortex sections displayed the normal structure of glomeruli with urinary space that is surrounded by visceral and parietal cells and displayed the normal structure of proximal tubules and distal tubules (Fig. 2a, b). Diabetic control animals displayed renal cortex with shrunk glomeruli and expanded urinary space, and also displayed severe degenerated renal tubules with pyknotic nuclei and completely demolished glomeruli and blood vessels with marked hyalinization and vacuolated cytoplasm (Fig. 2c, d). There was no ameliorative effect in diabetic kidney treated with CSNPs, whereas the renal cortex injury was represented by pyknotic nuclei and vacuoles (Fig. 2e). However, treatment with

POLY-CSNPs displayed a notable improvement in the glomeruli, distal, and proximal tubules appeared almost identical to that of the control (Fig. 2f), treating of diabetic rats with POLY illustrated moderate amelioration in the distal, proximal, and glomeruli tubules (Fig. 2g), and treating with METF displayed marked amelioration in the glomeruli, proximal, and distal tubules (Fig. 2h). Renal cortex sections of normal control rats stained by Masson's trichrome stain displayed normal few fine collagen fibers between tubules (Fig. 3a). The renal cortex of diabetic control animals indicated enormous deposition of the blue collagen fibers at the tubular lumen, in the tubular basement membrane, in interstitial areas, around the glomeruli, and around blood vessels (Fig. 3b). Diabetic rats administered with CSNPs showed marked blue collagenous fibers between the tubules and around blood vessels (Fig. 3c). POLY-CSNPs, POLY, and METF decreased the fibrosis of renal cortex in diabetic rat kidney tissues, whereas the diabetic group treated with POLY-CSNPs displayed disappearance of collagen fibers between tubules and around glomeruli (Fig. 3d), the diabetic group treated with POLY illustrated a reducing interstitial area collagen fibers (Fig. 3e) and diabetic rats that had received METF revealed a significant development such as an elimination in collagen fibers (Fig. 3f).

### 3.7 Immunohistochemical studies

Normal control rats' kidney sections stained by NF  $\kappa\beta$  and TNF  $\alpha$  stains displayed negative reactions (Figs. 4a, 5a). Regarding this research, the kidney of the diabetic control group (Figs. 4b; 5b) and diabetic rats administered with CSNPs (Figs. 4c, 5c) displayed intense brown positive immunoreaction in nuclei of renal cells for NF  $\kappa\beta$  and cytoplasm of renal cells for TNF  $\alpha$ , respectively. POLY-CSNPs demonstrated negative nucleic immunoreactions for NF  $\kappa\beta$  and negative cytoplasmic immune responses for TNF  $\alpha$ , respectively (Figs. 4d, 5d), whereas POLY showed moderate immunoreaction (Figs. 4e, 5e) and METF showed weak immunoreaction (Figs. 4f, 5f) for NF  $\kappa\beta$  and TNF  $\alpha$ , respectively. Notably, POLY-CSNPs demonstrated a significant reduction in the mean area percentage of NF  $\kappa\beta$  and TNF  $\alpha$  when compared to POLY (Additional file 1: Table S2).

### 3.8 Ultrastructural studies

Normal control kidney tissue ultrastructural observations displayed the normal structure of a glomerulus with podocytes with a large nucleus (Fig. 6a), normal basal lamina, and podocytes secondary foot processes (Fig. 6b). The normal structure of proximal tubules with euchromatic spherical nucleus, apical microvilli, normal-sized mitochondria (Fig. 6c). Kidney sections of diabetic control rats displayed glomerulus with degenerated podocytes (Fig. 6d), marked thickening of the basal lamina with a fusion of foot processes of podocytes and effacement of others (Fig. 6e). The proximal tubules appeared with swelling mitochondria, dark heterochromatin clumps adjacent to the nuclear membrane, marked degeneration of basal infoldings, and damage of microvilli (Fig. 6f). CSNP-treated diabetic rats displayed no improvement effects in diabetic rats, whereas it showed the glomerulus with degenerated podocytes (Fig. 7a), thickening of the basal lamina with effacement of foot processes of podocyte (Fig. 7b) and the proximal tubules with swelling mitochondria, damage of microvilli, and numbers of lysosomes (Fig. 7c). However, treatment with POLY-CSNPs demonstrated the nearly normal structure

of the glomerulus with podocytes (Fig. 7d), the basal lamina and foot processes of podocytes were more like the typical control animals (Fig. 7e) and the structure of proximal tubules was resembled the normal control group closely with spherical nucleus with euchromatin and heterochromatin, microvilli (Fig. 7h). Diabetic animals' treatment with POLY displayed improvement in the structure of a glomerulus and podocyte cell (Fig. 8a), improvement in the basal lamina and foot processes of podocytes (Fig. 8b), and the structure of proximal tubules with spherical nucleus with euchromatin and heterochromatin, microvilli (Fig. 8c). Treatment with METF revealed marked amelioration in the glomerulus with podocyte cell (Fig. 8d) and marked improvement in the basal lamina with podocytes foot processes (Fig. 8e), in addition to an obvious amelioration in the structure of the proximal tubules with spherical nucleus and microvilli (Fig. 8h).

## 4 Discussion

Long-term hyperglycemia in diabetes mellitus promotes the evolution of AGEs [46, 47], which are a part of diabetic complications pathogenesis as nephropathy [48]. The essential aim of diabetes care and nephropathy prevention is to keep blood glucose and redox levels normal (Fig. 9). The current findings indicated that one month of oral administration of POLY-CSNPs, POLY, and METF independently decreased elevated FBS levels and HbA1c %, suggesting anti-diabetic activity. The current results corroborate previous research that found hypoglycemic effects in POLY-CSNPs [27], POLY [49], and METF [50]. Since polydatin alleviated hyperuricemia-related diseases and alleviated damage to kidneys [51] and polydatin nanoparticles were more effective than polydatin in its anti-diabetic action, inhibition of oxidative stress status by boosting antioxidant enzymes, and modulation of pro-inflammatory cytokines [52]. AGEs accumulate in tissue, triggering target protein and lipid denaturation and functional decline, as well as organopathy [53]. In diabetic animals, however, body weight decreased, kidney weight increased and kidney biomarkers such

(See figure on next page.)

**Fig. 2** Photomicrograph of kidney cortex sections stained with H & E (**a** and **b**) C animals showing a glomeruli (G) normal structure with urinary space (S) which is lined by visceral (arrowhead) and parietal (arrow) cells. Proximal (PT) and distal (DT) tubules are also seen (**a**; scale bar = 100  $\mu\text{m}$  and **b**; scale bar = 50  $\mu\text{m}$ ), **c** and **d** D animals exhibiting renal cortex with shrunk glomeruli (G) and expanded urinary space (S). Severe degenerated renal tubules (arrows) with pyknotic nuclei (arrowhead) and completely demolished glomeruli (DG). Blood vessels with marked hyalinization (red arrow) and vacuolated cytoplasm (V) are also seen (**c**; scale bar = 100  $\mu\text{m}$  and **d**; scale bar = 50  $\mu\text{m}$ ), **e** D + CSNPs animals displaying renal cortex injury represented by marked degenerated renal tubules (asterisk), pyknotic nuclei and vacuoles (V) (scale bar = 50  $\mu\text{m}$ ), **f** D + POLY-CSNPs animals demonstrating significant amelioration in glomeruli (G), proximal (PT), and distal (DT) tubules appear nearly similar to that of the control (scale bar = 50  $\mu\text{m}$ ), **g** D + POLY animals demonstrating moderate amelioration glomeruli (G) in addition to proximal (PT) and distal (DT) tubules (scale bar = 50  $\mu\text{m}$ ), **h** D + METF animals illustrating amelioration in the glomeruli (G) in addition to proximal (PT) and distal (DT) tubules (scale bar = 50  $\mu\text{m}$ )



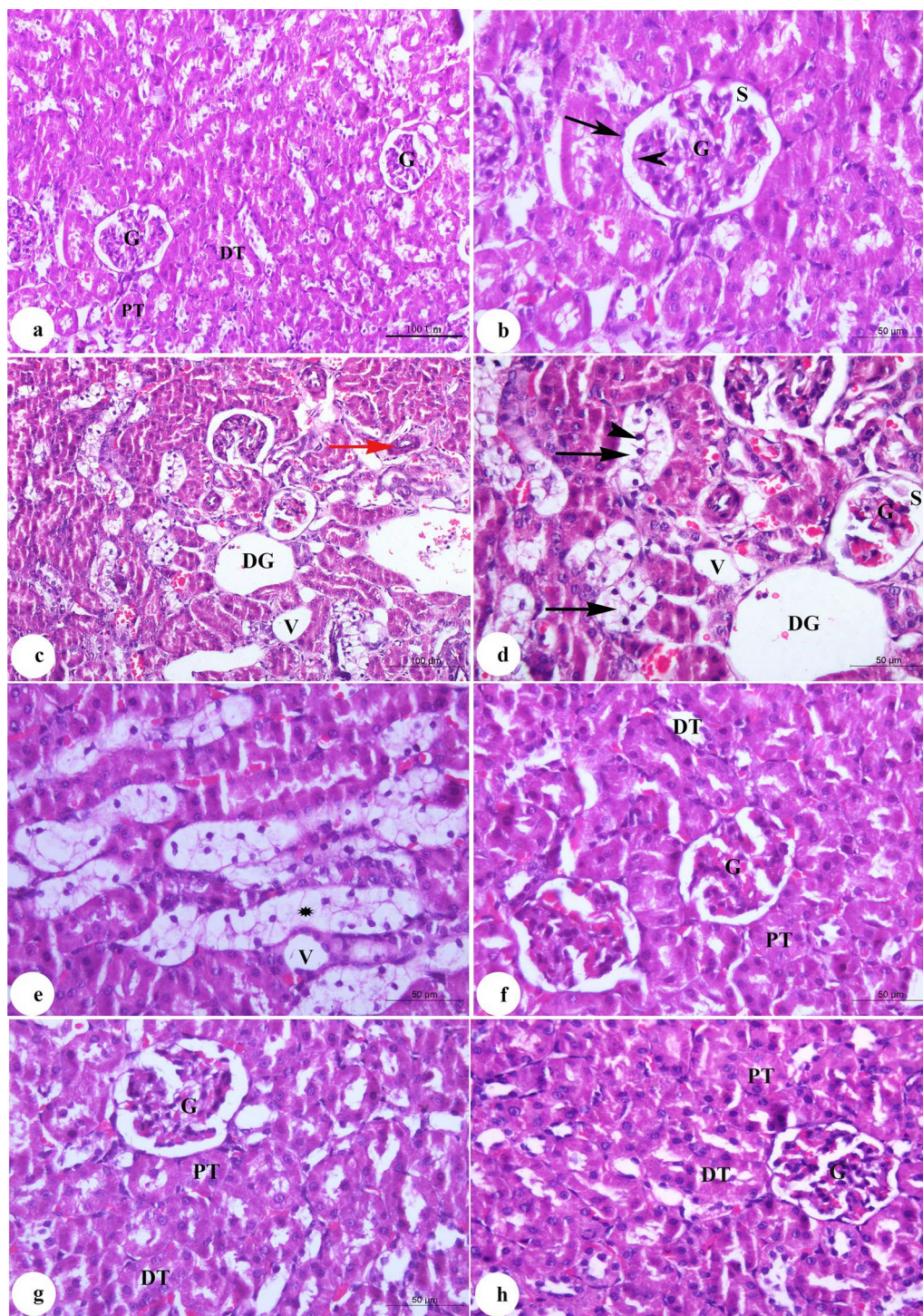


**Fig. 2** (See legend on previous page.)

as uric acid, creatinine, and urea increased [54]. The effects of POLY-CSNPs, POLY, and METF treatment on body weight loss, kidney weight gain, and kidney function increase in diabetic animals were found to be beneficial. This finding was confirmed by Niu et al., who

found that POLY protects diabetic rats from kidney injury [49], also METF could relieve renal injury in diabetic rats [55], and POLY-CSNPs had an anti-diabetic effect and increased the level of serum insulin of diabetic animals when compared to free polydatin which could

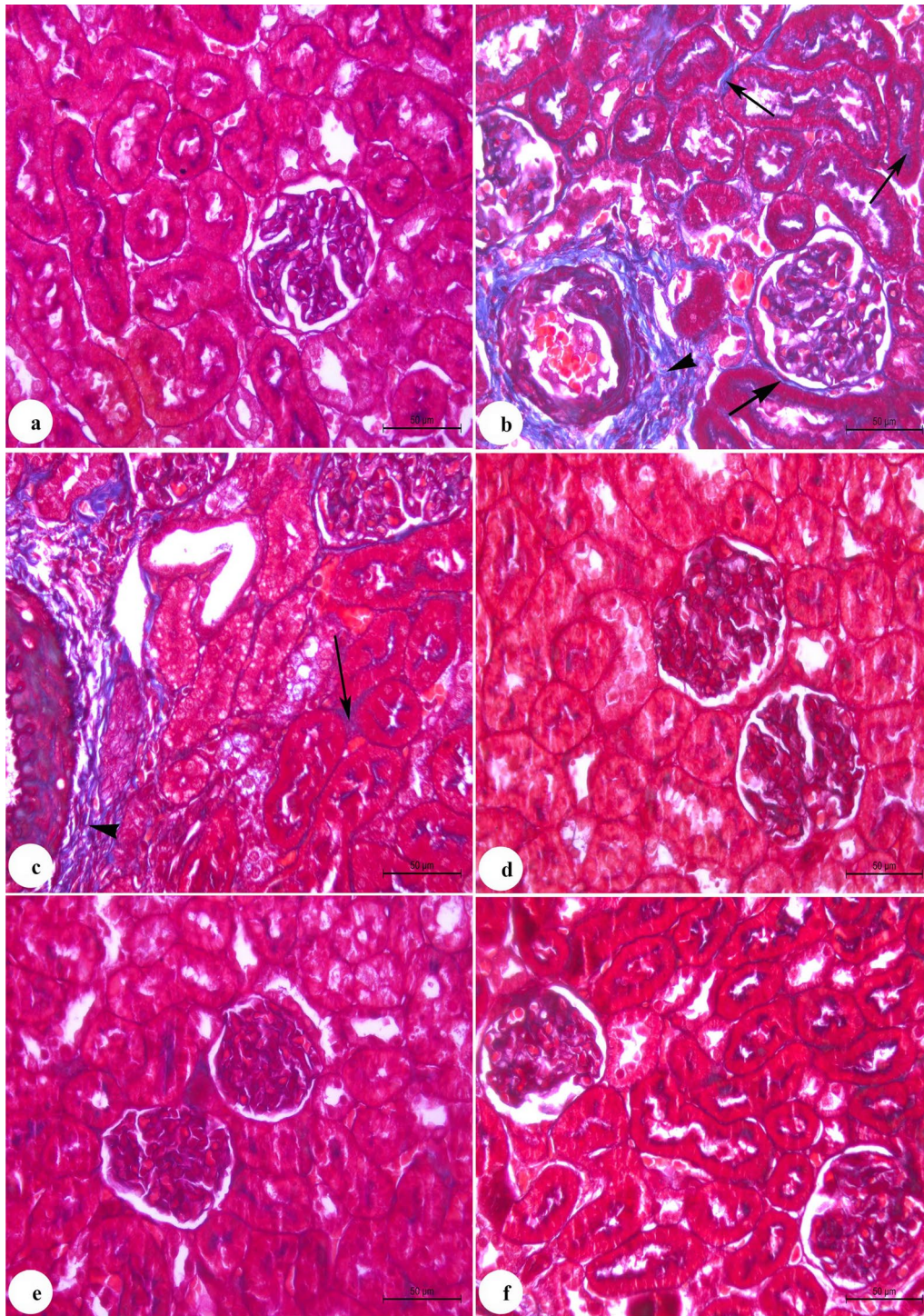


**Fig. 3** Photomicrograph of kidney cortex sections stained with Masson's trichrome **a** C animals with standard few fine collagen fibers between tubules (scale bar= 50  $\mu$ m), **b** D animals demonstrating the deposition of collagen fibers in a huge blue color at the tubular lumen, in tubular basement membrane, in interstitial areas, around the glomeruli (arrows) and around blood vessels (arrowhead) (scale bar= 50  $\mu$ m), **c** D+CSNPs animals displaying collagen fibers in a marked blue color between tubules (arrow) and around blood vessels (arrowhead) (scale bar= 50  $\mu$ m), **d** D+POLY-CSNPs animals displaying collagen fibers invisibility between tubules and around glomeruli (scale bar= 50  $\mu$ m), **e** D+POLY animals showing reducing of interstitial area collagen fibers (scale bar= 50  $\mu$ m), **f** D+METF animals illustrating a significant improvement as well as collagen fibers reduction (scale bar= 50  $\mu$ m)

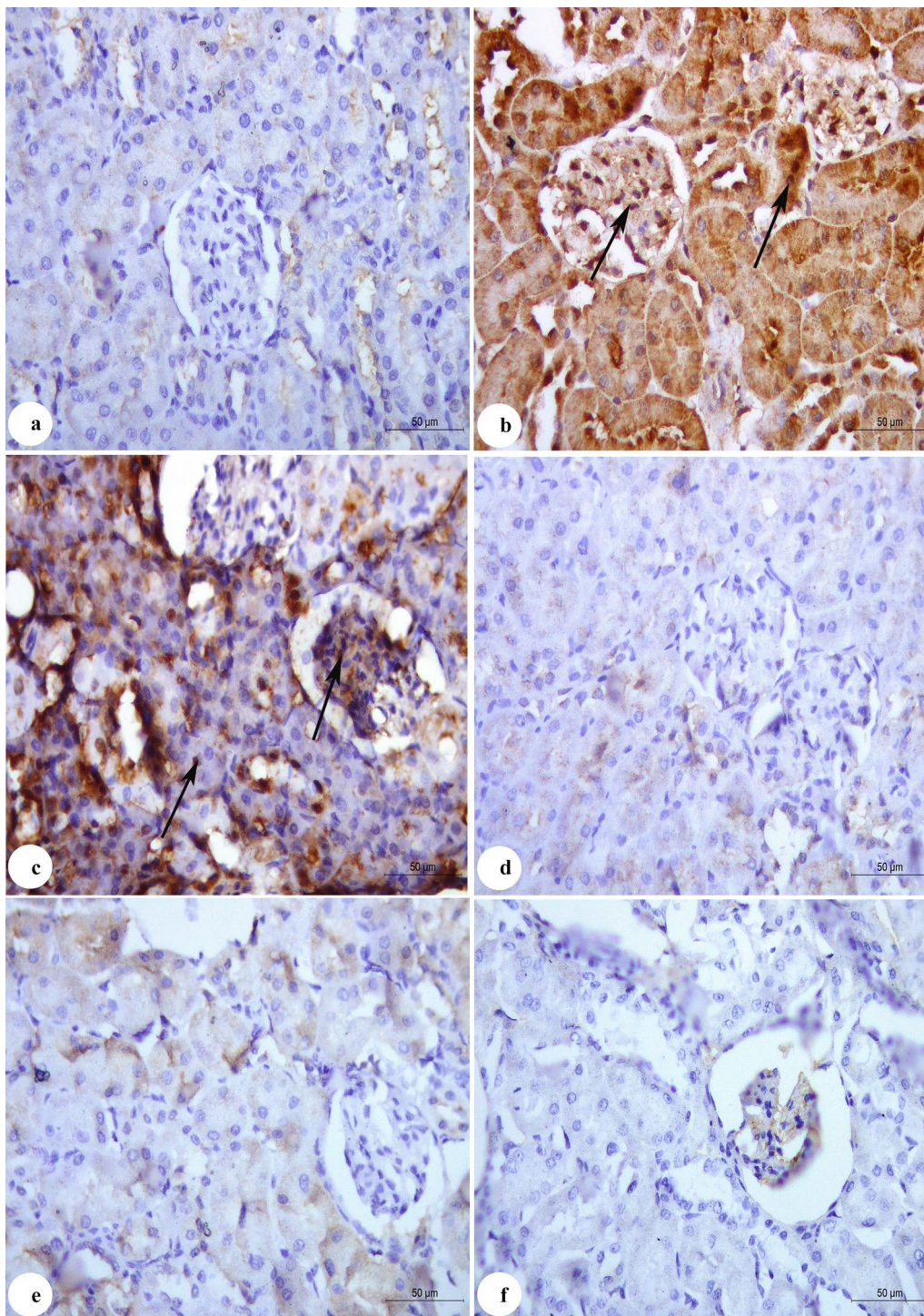


**Fig. 4** Photomicrograph of kidney cortex sections stained with NF  $\kappa\beta$  **a** C animals displaying negative immune response (scale bar = 50  $\mu\text{m}$ ), **b** D animals demonstrating positive immune response represented by dark brown color in renal cells nuclei (arrows) (scale bar = 50  $\mu\text{m}$ ), **c** D+CSNPs animals demonstrating nuclei positive immune response (arrows) (scale bar = 50  $\mu\text{m}$ ), **d** D+POLY-CSNPs animals demonstrating negative immune response (scale bar = 50  $\mu\text{m}$ ), **e** D+POLY animals demonstrating moderate immune response (scale bar = 50  $\mu\text{m}$ ), **f** D+METF animals demonstrating weak immune response (scale bar = 50  $\mu\text{m}$ )

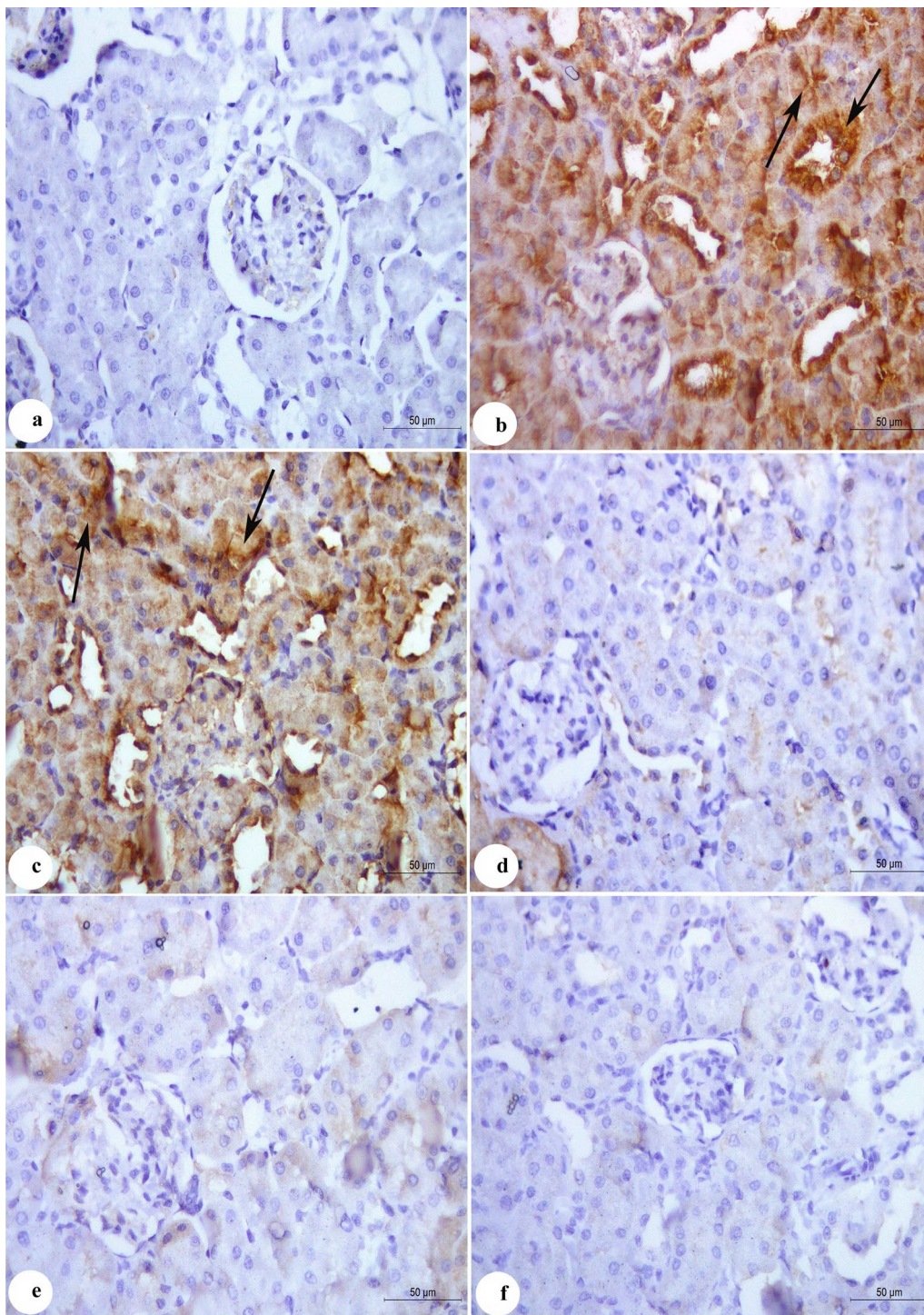


**Fig. 5** Photomicrograph of kidney cortex sections stained with TNF  $\alpha$  **a** C animals displaying negative response (scale bar = 50  $\mu$ m), **b** D animals displaying strong positive dark brown color in renal cell cytoplasm (arrows) (scale bar = 50  $\mu$ m), **c** D + CSNPs animals displaying cytoplasm positive immune response (arrows) (scale bar = 50  $\mu$ m), **d** D + POLY-CSNPs animals demonstrating negative immune response (scale bar = 50  $\mu$ m) **e** D + POLY animals displaying moderate immune response (scale bar = 50  $\mu$ m), **f** D + METF animals revealing few immune response (scale bar = 50  $\mu$ m)

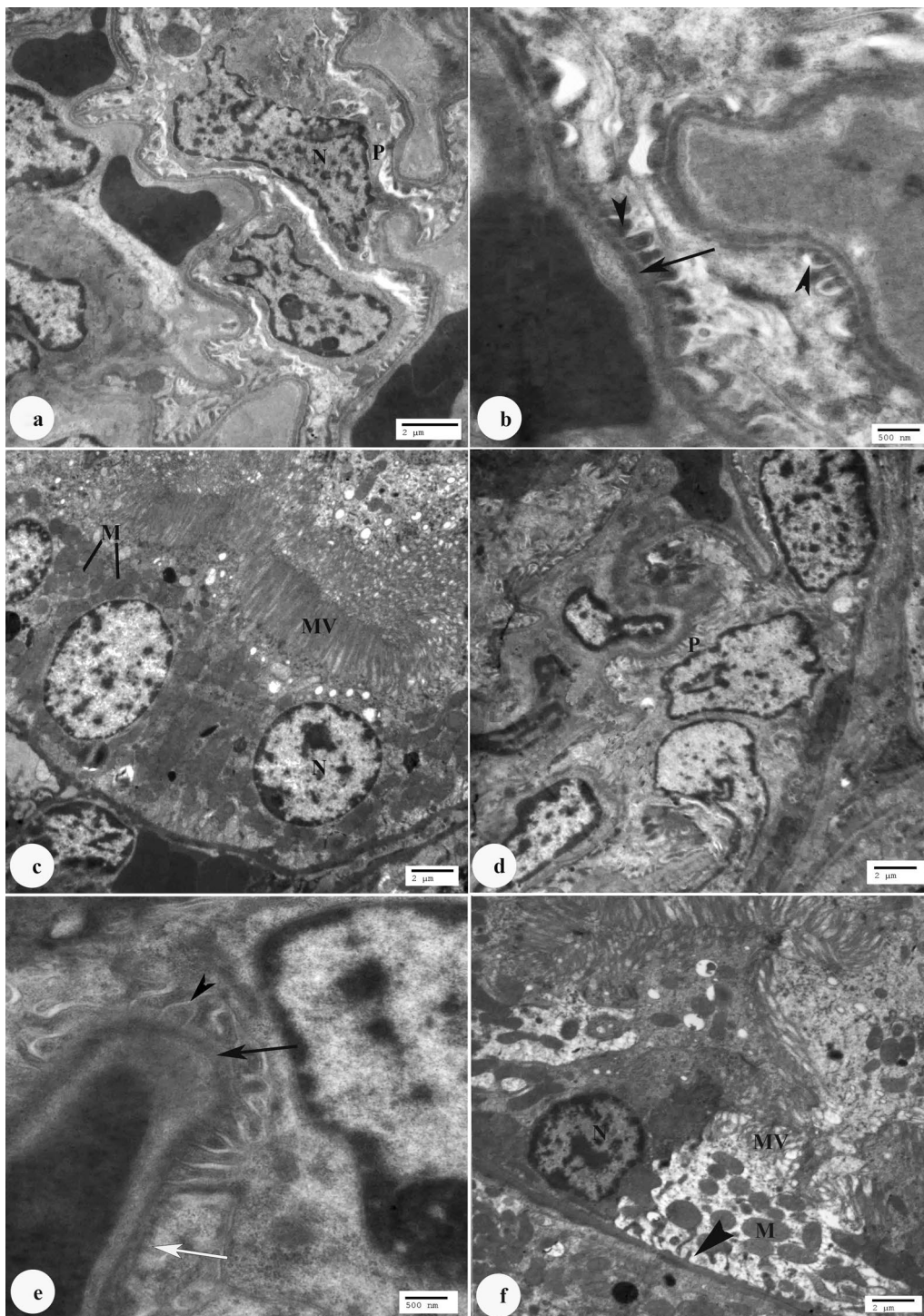


**Fig. 6** Electron micrograph of kidney cortex section **a:** C animals demonstrating the normal structure of a glomerulus with podocytes (P) with large nucleus (N) (scale bar = 2 μm), **b:** C animals showing normal basal lamina (arrow) and secondary foot processes of podocytes (arrowheads) (scale bar = 500 nm), **c:** C animals showing normal structure of the proximal tubules with euclromatic spherical nucleus (N), apical microvilli (MV), normal size of mitochondria (M) (scale bar = 2 μm), **d:** D animals demonstrating glomerulus with degenerated podocytes (P) (scale bar = 2 μm), **e:** D animals demonstrating marked thickening of the basal lamina (arrow) with fusion of foot processes of podocytes (arrowhead) and effacement of others (white arrow) (scale bar = 500 nm), **f:** D animals showing the proximal tubules with swelling mitochondria (M), a nucleus with dark heterochromatin clumps adjacent to nuclear membrane (N) and marked degeneration of basal infoldings (arrowhead) and damage of microvilli (MV) (scale bar = 2 μm)

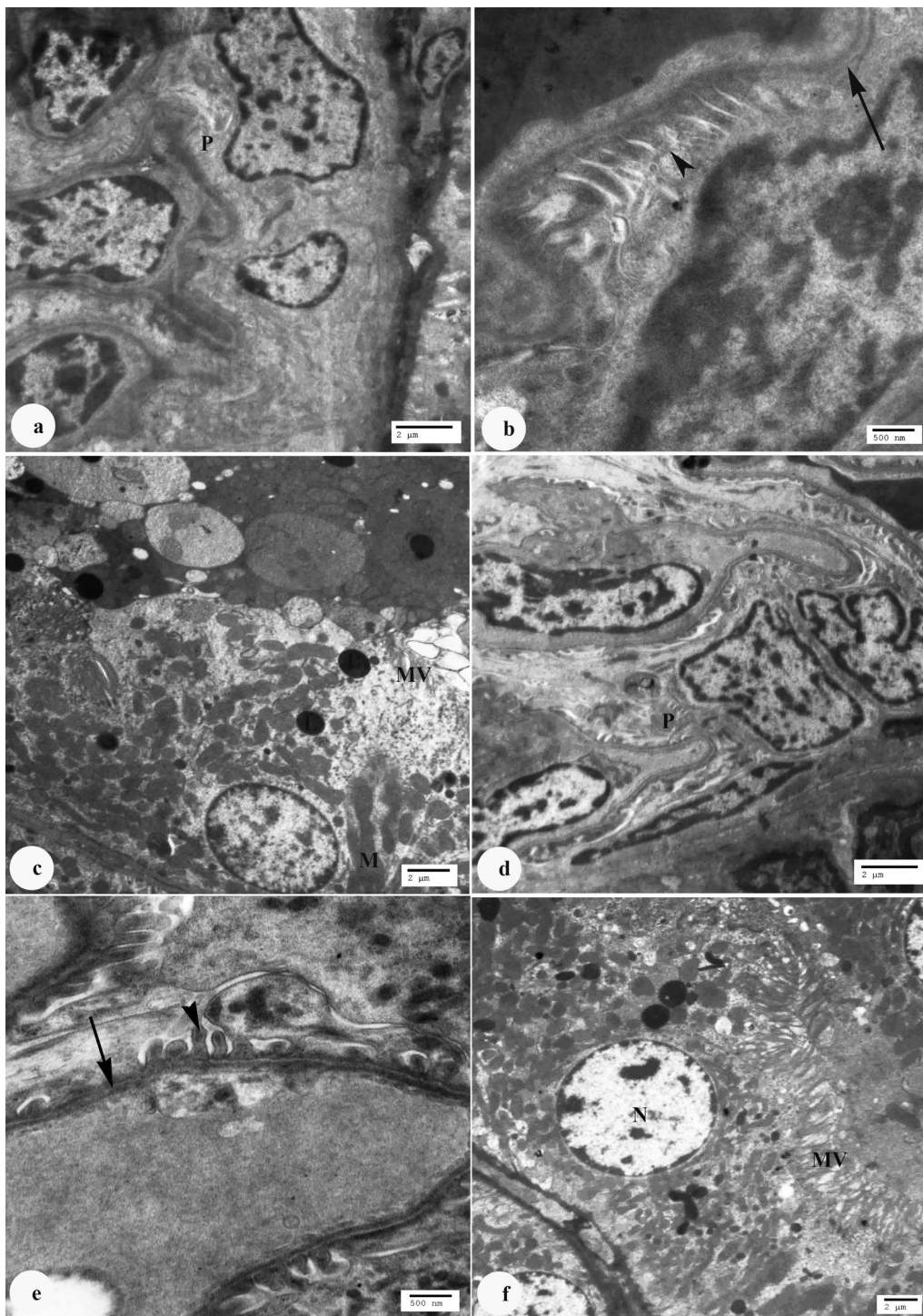


**Fig. 7** Electron micrograph of kidney section **a** D+CSNPs animals demonstrating glomerulus with degenerated podocytes (P) (scale bar=2  $\mu$ m), **b** D+CSNPs animals demonstrating thickening of the basal lamina (arrow) with effacement of foot processes of podocyte (arrowhead) (scale bar=500 nm), **c** D+CSNPs animals demonstrating the proximal tubules with swelling mitochondria (M), damage of microvilli (MV) and numbers of lysosomes (L) (scale bar=2  $\mu$ m), **d** D+POLY-CSNPs animals demonstrating the glomerulus is more like the typical control animals with podocytes (P) (scale bar=2  $\mu$ m), **e** D+POLY-CSNPs animals demonstrating the basal lamina (arrow) and foot processes of podocytes (arrowhead) are more like the typical control animals (scale bar=500 nm), **f** D+POLY-CSNPs animals demonstrating nearly normal proximal tubules with spherical nucleus (N) with euchromatin and heterochromatin and microvilli (MV) (scale bar=2  $\mu$ m)

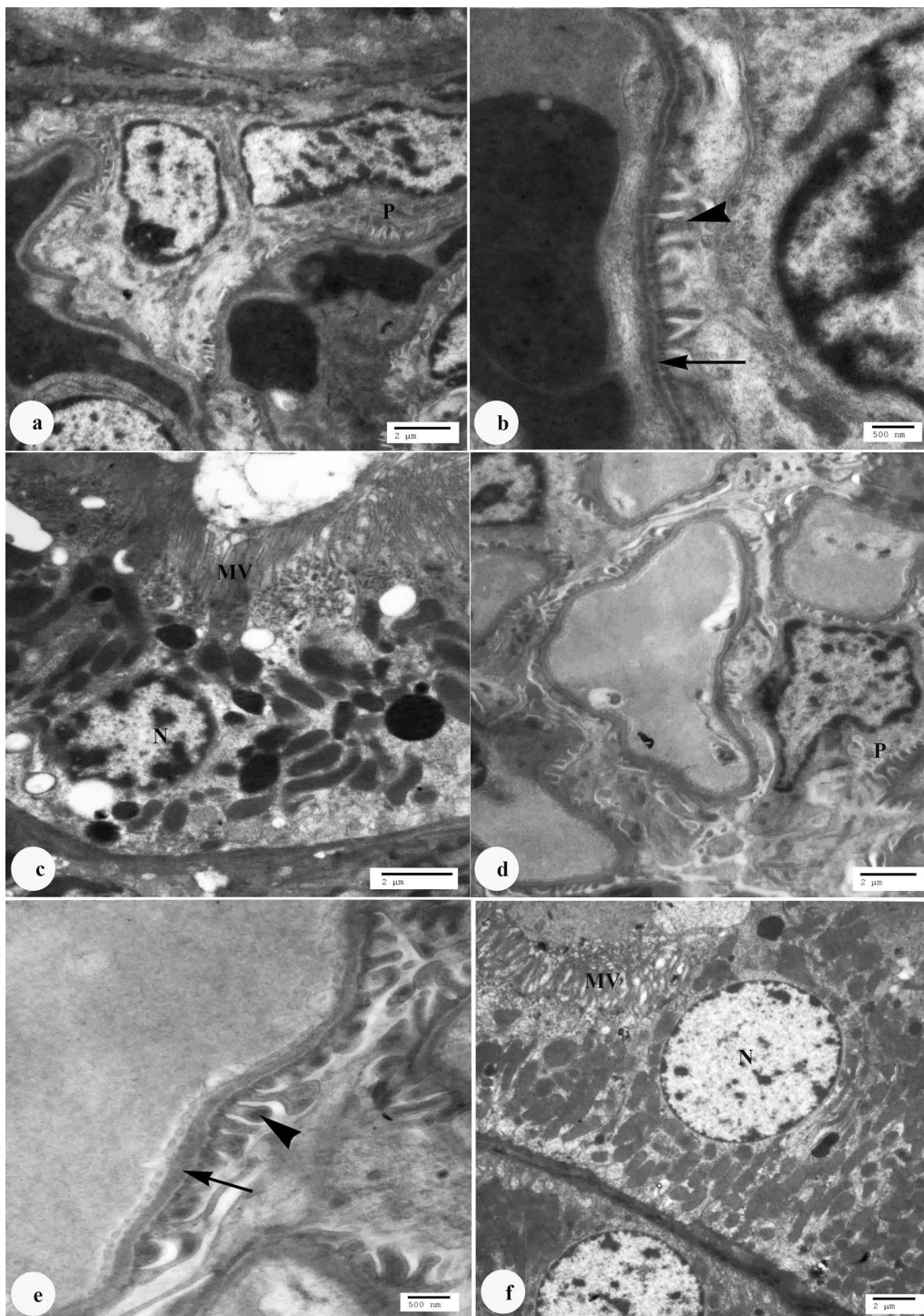


**Fig. 8** Electron micrograph of kidney section **a** D+POLY animals demonstrating improvement in the structure of a glomerulus and podocyte cell (P) (scale bar = 2  $\mu$ m), **b** D+POLY animals demonstrating the basal lamina (arrow) and foot processes of podocytes (arrowhead) are improved (scale bar = 500 nm), **c** D+POLY animals demonstrating amelioration in the structure of the proximal tubules with spherical nucleus (N) with euchromatin and heterochromatin, microvilli (MV) (scale bar = 2  $\mu$ m), **d** D+METF animals demonstrating marked amelioration in glomerulus with podocyte cell (P) (scale bar = 2  $\mu$ m), **e** Animals treated with D+METF demonstrating significant improvement in the basal lamina (arrow) with foot processes of podocytes (arrowhead) (scale bar = 500 nm), **f** D+METF animals demonstrating the structure of the proximal tubules with spherical nucleus (N) and microvilli (MV) is markedly improved (scale bar = 2  $\mu$ m)

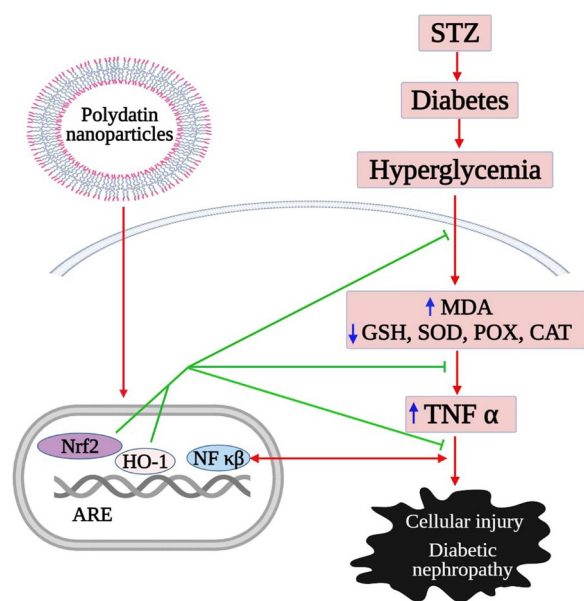


**Fig. 9** A diagram summarized the probable mechanism of polydatin nanoparticles for alleviating diabetic nephropathy. STZ: streptozotocin; MDA: lipid peroxides; GSH: reduced glutathione concentration; SOD: superoxide dismutase activity; POX: peroxidase activity; CAT: catalase activity; TNF  $\alpha$ : tumor necrosis factor alpha; NF  $\kappa\beta$ : nuclear factor-kappa  $\beta$ ; Nrf2: nuclear factor erythroid 2-related factor 2; HO-1: heme oxygenase-1; ARE: antioxidant response elements

be attributed to their capabilities for longer release and enhanced absorption [27].

Hyperglycemia results in redox imbalance and excessive ROS generation, leading to mitochondrial malfunction and macromolecule oxidation, which speeds up apoptosis and disease progression [56]. Excess intracellular glucose damages renal tissue, contributing to the intense oxidation that promotes the death of cells [46, 57], while the interaction of AGEs with their receptor triggers the markers of oxidative stress, heme oxygenase, and NF  $\kappa\beta$  [58]. Oxidative stress is caused by a disparity between the generation of free radicals and the scavenging of antioxidant mechanisms [56]. In the diabetic group, MDA was significantly increased, NF  $\kappa\beta$  revealed positive immunoreactions in renal cell nuclei and TNF  $\alpha$  revealed positive immunoreactions in the renal cell cytoplasm. TNF  $\alpha$  causes the resistance of insulin because it is one of the most prevalent catalysts for NF  $\kappa\beta$  expression and is a cytoplasm pro-inflammatory cytokine [59]. Active NF  $\kappa\beta$  expression causes  $\beta$ -cell death via cytokine-induced cell death [60]. Increased ROS activates the response elements of antioxidants (ARE), which allow antioxidant genes to be induced to protect cells from oxidative stress [61, 62]. Since GSH, CAT, SOD, and POX are the initial line of cellular protection for oxidative

stress [63], the number of enzymatic antioxidants such as GSH, SOD, CAT, and POX decreased in diabetic rats. Via binding to and triggering the expression of antioxidant response factor promoters, Nrf2 is a transcription factor important in the complex regulation of a network of cytoprotective genes and antioxidants [64]. Therefore, the activation of Nrf2 regulates the antioxidant protein expression that preserves cells from oxidative harm induced by inflammation and injury [65]; also, it inhibits NF  $\kappa\beta$  activation and induces HO-1 cytoprotective protein [66]. Thus, in diabetic rats, Nrf2 and HO-1 signaling pathway dysfunction was discovered in this study. In diabetic rats, however, oral administration of POLY-CSNPs, POLY, and METF decreased lipid peroxidation products and gene expression (NF- $\kappa\beta$  and TNF- $\alpha$ ) by increasing enzymatic antioxidant activities as GSH, SOD, CAT, and POX, also rising the expression of HO-1 and Nrf2. POLY nanoparticles have antioxidant activity and anti-lipid peroxidation [67]. POLY protects against DN by reducing inflammatory reactions and preventing cell death, at least in part, by turning off the pathway of TLR4/NF- $\kappa\beta$  [49]. The treatment with METF decreased the oxidative stress activation and improved the function of mitochondria by the activation of Nrf2 transcription and binding to ARE [68], additionally lowering TNF- $\alpha$  and NF- $\kappa\beta$  levels [69].

Biochemical and immunohistochemical results were confirmed by histopathological kidney examinations. Diabetic kidney tissues showed a renal cortex with shrunk glomeruli and expanded urinary space [70]. Also, diabetic kidneys displayed severe degenerated renal tubules with pyknotic nuclei and completely demolished glomeruli and blood vessels with marked hyalinization and vacuolated cytoplasm and collagen fibers deposition at the tubular lumen, in the tubular basement membrane, in interstitial areas, around the glomeruli and blood vessels [71]. Such pathological alterations are consistent with the previous research that showed oxidative stress's negative impacts on the kidneys of diabetic rats [72]. The kidney architecture of diabetic rats was preserved after treatment with POLY-CSNPs, POLY, and METF, according to the findings. This may be because of their antioxidant, anti-apoptotic, and anti-inflammatory properties. POLY attenuates the oxidative stress of the kidney and reduces the diabetic renal fibrosis progression [73–75]. METF, on the other hand, reduces glycolipid metabolism disorders, kidney function damage in rats with diabetes, and oxidative stress, implying a metformin-protecting function for the pathological mechanism of diabetic kidney disease [30].

Diabetes caused changes in the kidney, whereas the diabetic kidneys showed glomerulus with degenerated podocytes, thickening of the basal lamina with a fusion of foot processes of podocytes, and effacement of others.



Proximal tubules with swelling mitochondria, a nucleus with dark heterochromatin clumps, adjust to the nuclear membrane, and degeneration of basal infoldings and damage of microvilli. As compared to standard GBM, the glomerular basement membrane is diffusely thickened and the tubular basement membrane is thickened [76, 77]. Administration of POLY-CSNPs, POLY, and METF had a major ameliorative effect in diabetic rats relative to untreated diabetic rats, implying that POLY-CSNPs, POLY, and METF treatment would prevent diabetic kidney tissue ultrastructural alterations in this animal model. Treatment with POLY prevented mesangial expansion and preserved normal glomerular structure, and the podocin and nephrin protein levels also normalized the foot processes' shape and the slit pores of podocyte [78]. In diabetic rats, METF decreased the glomerular basement membrane's thickness and prevented foot process fusion [55, 70].

Although the present study succeeded in revealing the protective impact of polydatin nanoparticles for diabetic nephropathy, the study had some limitations. Firstly, a lack of estimation of more anti-inflammatory and inflammatory biomarkers could affect inflammation and pathogenesis processes related to diabetic nephropathy. Finally, the study was not subject to the testing insulin-treated group for comparison with other treated groups as well as assessing urine albumin/creatinine ratio.

## 5 Conclusion

Since CSNPs were a possible nano-carrier for sustained delivery of POLY, POLY-CSNPs as a new formula showed a strong anti-diabetic and kidney-protective efficacy when compared to POLY and METF. As a result, POLY-CSNPs are effective and significant in protecting diabetic rats' kidneys from nephropathy by lowering NF- $\kappa$ B and TNF- $\alpha$  levels in the kidneys and promoting the HO-1/Nrf2 signaling pathway. In rats with diabetes, POLY-CSNPs markedly reduce the biomarkers of oxidative stress, ultrastructural, and histopathological alterations when compared to free POLY. Therefore, POLY-CSNPs formula may serve as a potential improvement over the current POLY treatment for type 2 diabetes.

### Abbreviations

ROS	Reactive oxygen species
DN	Diabetic nephropathy
NF $\kappa$ B	Nuclear factor-kappa beta
Nrf2	Nuclear factor erythroid 2-related factor 2
TNF $\alpha$	Tumor necrosis factor alpha
POLY	Polydatin
CS	Chitosan
TPP	Triphosphosphate

METF	Metformin
ADA	American Diabetes Association
PB	Phosphate buffer
T2DM	Type 2 diabetes mellitus
AGEs	Advanced glycation end products
DNA	Deoxyribonucleic acid
HO-1	Heme oxygenase-1
SOD	Superoxide dismutase
ARE	Antioxidant responsive element
MDA	Malondialdehyde in lipid peroxidation
CAT	Catalase
RNA	Ribonucleic acid
H <sub>2</sub> O <sub>2</sub>	Hydrogen peroxide
POX	Peroxidase activity
GSH	Reduced glutathione content
Fig	Figure
TLR4	Toll-like receptor4
STZ	Streptozotocin
NA	Nicotinamide
METF	Metformin hydrochloride
CMC	Carboxymethyl cellulose
FBG	Fasting blood glucose
HbA1c	Glycosylated hemoglobin
HCl	Hydrochloric acid
POLY-CSNPs	Polydatin-loaded chitosan nanoparticles
CSNPs	Chitosan nanoparticles
C	Control
D	Diabetic

## Supplementary Information

The online version contains supplementary material available at <https://doi.org/10.1186/s43088-023-00441-1>.

**Additional file 1. Table S1.** Effect of POLY-CSNPs, POLY and METF on urea, creatinine, uric acid, MDA, GSH, SOD, POX, CAT, Nrf2 and HO-1 in the studied groups. **Fig. S1.** Nrf2: nuclear factor erythroid 2-related factor 2; HO-1: heme oxygenase-1 of normal control animals (C), diabetic control group (D), diabetic animals-treated with blank chitosan nanoparticles (D+CSNPs), diabetic group-treated with polydatin loaded chitosan nanoparticles (D+POLY-CSNPs), polydatin (D+POLY) and metformin-HCL (D+METF) respectively for 4 weeks. Data are expressed as mean  $\pm$  SEM (n = 6). ###P <0.001 versus control; \*P <0.05, \*\*P <0.01 and \*\*\*P <0.001 versus diabetic control. **Table S2.** The mean area percentage of NF- $\kappa$ B and TNF- $\alpha$  immunostaining of all studied groups.

### Acknowledgements

Not applicable.

### Author contributions

All authors have contributed significantly. NM, MA, and KA have contributed in suggesting the design of the work, preparation and analysis of the results, and interpretation of data and discussion. In addition, AM has performed the practical part. All authors are in agreement with the contents of the manuscript. All authors read and approved the final manuscript.

### Funding

Not applicable.

### Availability of data and materials

The authors confirmed that all data generated or analyzed during this study are included in this published article.

### Declarations

#### Ethics approval and consent to participate

All animal procedures were conducted in accordance with the standards set forth in the guidelines for the care and use of experimental animals by the

Animal Ethics Committee of the Zoology Department in the Faculty of Science at Beni-Suef University (Ethical Approval Number: BS-FS-2018-14).

#### Consent for publication

Not applicable.

#### Competing interests

The authors declare that they have no competing interests.

#### Author details

<sup>1</sup>Histology and Cytology Division, Zoology Department, Faculty of Science, Beni-Suef University, Salah Salem St., P.O. Box 62521, Beni-Suef 62511, Egypt. <sup>2</sup>Genetic and Molecular Genetic Division, Zoology Department, Faculty of Science, Beni-Suef University, Beni-Suef, Egypt. <sup>3</sup>Molecular Physiology Division, Zoology Department, Faculty of Science, Beni-Suef University, Beni-Suef, Egypt.

Received: 20 July 2023 Accepted: 30 October 2023

Published online: 06 November 2023

#### References

- Kittell F (2012) Diabetes management. In: Thomas LK, Othersen JB (eds) Nutrition therapy for chronic kidney disease. CRC Press, Boca Raton, p 198
- Wu T, Ding L, Andoh V, Zhang J, Chen L (2023) The mechanism of hyperglycemia-induced renal cell injury in diabetic nephropathy disease: an update. *Life (Basel)*. 13(2):539. <https://doi.org/10.3390/life13020539>
- Johansen KL, Chertow GM, Foley RN, Gilbertson DT, Herzog CA, Ishani A, Israni AK, Ku E, Kurella Tamura M, Li S, Li S, Liu J, Obrador GT, O'Hare AM, Peng Y, Powe NR, Roetker NS, St Peter WL, Abbott KC, Chan KE, Schulman IH, Snyder J, Solid C, Weinhandl ED, Winkelmayer WC, Wetmore JB (2021) US renal data system 2020 annual data report: epidemiology of kidney disease in the United States. *Am J Kidney Dis* 77(4 Suppl 1):A7–A8. <https://doi.org/10.1053/j.ajkd.2021.01.002>
- Saran R, Li Y, Robinson B, Abbott KC, Agodoa LY, Ayanian J, Bragg-Gresham J, Balkrishnan R, Chen JL, Cope E, Eggers PW, Gillen D, Gipson D, Hailpern SM, Hall YN, He K, Herman W, Heung M, Hirth RA, Hutton D, Jacobsen SJ, Kalantar-Zadeh K, Kovesdy CP, Lu Y, Molnar MZ, Morgenstern H, Nallamothu B, Nguyen DV, O'Hare AM, Plattner B, Pisoni R, Port FK, Rao P, Rhee CM, Sakhuja A, Schaubel DE, Selewski DT, Shahinian V, Sim JJ, Song P, Streja E, Kurella Tamura M, Tentori F, White S, Woodside K, Hirth RA (2016) US renal data system 2015 annual data report: epidemiology of kidney disease in the United States. *Am J Kidney Dis* 67(3):S1–305. <https://doi.org/10.1053/j.ajkd.2015.12.014>
- Reich H, Tritchler D, Herzenberg AM, Kassiri Z, Zhou X, Gao W, Scholey JW (2005) Albumin activates ERK via EGF receptor in human renal epithelial cells. *J Am Soc Nephrol* 16(5):1266–1278. <https://doi.org/10.1681/ASN.2004030222>
- Whaley-Connell AT, Morris EM, Rehmer N, Yaghoubian JC, Wei Y, Hayden MR, Habibi J, Stump CS, Sowers JR (2007) Albumin activation of NAD(P) H oxidase activity is mediated via Rac1 in proximal tubule cells. *Am J Nephrol* 27(1):15–23. <https://doi.org/10.1159/000098432>
- Diwakar R, Pearson AL, Colville-Nash P, Brunskill NJ, Dockrell ME (2007) The role played by endocytosis in albumin-induced secretion of TGF-beta1 by proximal tubular epithelial cells. *Am J Physiol Renal Physiol* 292(5):F1464–F1470. <https://doi.org/10.1152/ajprenal.00069.2006>
- Roscioni SS, Lambers Heerspink HJ, de Zeeuw D (2014) Microalbuminuria: target for renoprotective therapy PRO. *Kidney Int* 86(1):40–49. <https://doi.org/10.1038/ki.2013.490>
- Koral K, Erkan E (2012) PKB/Akt partners with Dab2 in albumin endocytosis. *Am J Physiol Renal Physiol* 302(8):F1013–F1024. <https://doi.org/10.1152/ajprenal.00289.2011>
- Suryavanshi SV, Kulkarni YA (2017) NF- $\kappa$ B: a potential target in the management of vascular complications of diabetes. *Front Pharmacol* 8:798. <https://doi.org/10.3389/fphar.2017.00798>
- Patel S, Santani D (2009) Role of NF- $\kappa$ B in the pathogenesis of diabetes and its associated complications. *Pharmacol Rep* 61(4):595–603. [https://doi.org/10.1016/S1734-1140\(09\)70111-2](https://doi.org/10.1016/S1734-1140(09)70111-2)
- Koike N, Takamura T, Kaneko S (2007) Induction of reactive oxygen species from isolated rat glomeruli by protein kinase C activation and TNF- $\alpha$  stimulation, and effects of a phosphodiesterase inhibitor. *Life Sci* 80(18):1721–1728. <https://doi.org/10.1016/j.lfs.2007.02.001>
- Al-Qudah MMA, Al-Ramamneh ED, Moawiya A, Haddad AA (2018) The histological effect of aqueous ginger extract on kidneys and lungs of diabetic rats. *Int J Biol* 10(4):22–28. <https://doi.org/10.5539/ijb.v10n4p23>
- Bella LM, Fieri I, Tessaro FHG, Nolasco EL, Nunes FPB, Ferreira SS, Azevedo CB, Martins JO (2017) Vitamin D modulates hematological parameters and cell migration into peritoneal and pulmonary cavities in alloxan-diabetic mice. *Bio Med Res Int* 2017:7651815. <https://doi.org/10.1155/2017/7651815>
- Rezk HM, El-Sherbiny M, Atef H, Taha M, Hamdy S, Bedir RF (2017) Effect of spirinolactone on diabetic nephropathy in albino rats: ultrastructural and immunohistochemical study. *Int J Sci Rep* 3(5):110–119. <https://doi.org/10.18203/issn.2454-2156.IntJSciRep20171997>
- Sun L, Dutta RK, Xie P, Kanwar YS (2019) Withdrawal: myo-Inositol oxygenase overexpression accentuates generation of reactive oxygen species and exacerbates cellular injury following high glucose ambience: a new mechanism relevant to the pathogenesis of diabetic nephropathy. *J Biol Chem* 294(26):10380. <https://doi.org/10.1074/jbc.W119.009586>
- Mecwan M, Falcone N, Najafabadi AH, Khorsandi D (2023) Antioxidant Activity. *Am Chem Soc* 1438(5):71–80. <https://doi.org/10.1021/bk-2023-1438.ch005>
- Miulski D, Molski M (2010) Quantitative structure-antioxidant activity relationship of trans-resveratrol oligomers, trans-4,4'-dihydroxystilbene dimer, trans-resveratrol-3-O-glucuronide, glucosides: trans-piceid, cis-piceid, trans-astringin and trans-resveratrol-4'-O-beta-D-glucopyranoside. *Eur J Med Chem* 45(6):2366–2380. <https://doi.org/10.1016/j.ejmech.2010.02.016>
- Selvakumar G, Venu D, Kuttalam I, Lonchin S (2021) Inhibition of advanced glycation end product formation in rat tail tendons by polydatin and p-coumaric acid: an in vitro study. *Appl Biochem Biotechnol*. <https://doi.org/10.1007/s12010-021-03762-y>
- Jayalakshmi P, Devika PT (2019) Assessment of in vitro antioxidant activity study of polydatin. *J Pharmacognosy Phytochem* 8(4):55–58
- Park B, Jo K, Lee TG, Hyun SW, Kim JS, Kim CS (2019) Polydatin inhibits NLRP3 inflammasome in dry eye disease by attenuating oxidative stress and inhibiting the NF- $\kappa$ B pathway. *Nutrients* 11(11):2792. <https://doi.org/10.3390/nu11112792>
- Xu XH, Zheng N (2018) Polydatin protects diabetic nephropathy rats from renal inflammation by regulating the TLR4/NF- $\kappa$ B signal pathway. *Chin J Hospital Pharm* 38(16):1677–1680
- Wang L, Huang L, Li N, Miao J, Liu W, Yu J (2019) Ameliorative effect of polydatin on hyperglycemia and renal injury in streptozotocin-induced diabetic rats. *Cell Mol Biol* 65(7):55–59
- Cheng W, Li X, Zhang C, Chen W, Yuan H, Xu S (2017) Preparation and in vivo-in vitro evaluation of polydatin-phospholipid complex with improved dissolution and bioavailability. *Int J Drug Dev Res* 9:39–43
- Wong CY, Al-Salami H, Dass CR (2017) Potential of insulin nanoparticle formulations for oral delivery and diabetes treatment. *J Control Release* 264:247–275. <https://doi.org/10.1016/j.jconrel.2017.09.003>
- Yu Y, Gao J, Jiang L, Wang J (2021) Antidiabetic nephropathy effects of synthesized gold nanoparticles through mitigation of oxidative stress. *Arabian J Chem* 14(3):103007. <https://doi.org/10.1016/j.arabjc.2021.103007>
- Abdel-Moneim A, El-Shahawy A, Yousef AI, Abd El-Twab SM, Elden ZE, Taha M (2020) Novel polydatin-loaded chitosan nanoparticles for safe and efficient type 2 diabetes therapy: in silico, in vitro and in vivo approaches. *Int J Biol Macromol* 154:1496–1504. <https://doi.org/10.1016/j.ijbiomac.2019.11.031>
- Gnudi L, Ricciardi CA (2022) Diabetes and Kidney disease: metformin. In: Lerma EV, Batuman V (eds) Diabetes and kidney disease. Springer, Cham. [https://doi.org/10.1007/978-3-030-86020-2\\_24](https://doi.org/10.1007/978-3-030-86020-2_24)
- American Diabetes Association (ADA) (2009) Standards of medical care in diabetes—2009. *Diabetes Care* 32(1):S13–S61. <https://doi.org/10.2337/dc09-S013>
- Ren H, Shao Y, Wu C, Ma X, Lv C, Wang Q (2020) Metformin alleviates oxidative stress and enhances autophagy in diabetic kidney disease via AMPK/SIRT1-FoxO1 pathway. *Mol Cell Endocrinol* 500:110628. <https://doi.org/10.1016/j.mce.2019.110628>
- Nagpal K, Singh SK, Mishra DN (2013) Optimization of brain targeted chitosan nanoparticles of Rivastigmine for improved efficacy and safety.

- Int J Biol Macromol 59:72–83. <https://doi.org/10.1016/j.jbiomac.2013.04.024>
32. Soufi FG, Mohammad-Nejad D, Ahmadi H (2012) Resveratrol improves diabetic retinopathy possibly through oxidative stress—nuclear factor  $\kappa\beta$ —apoptosis pathway. *Pharmacol Rep* 64(6):1505–1514. [https://doi.org/10.1016/s1734-1140\(12\)70948-9](https://doi.org/10.1016/s1734-1140(12)70948-9)
  33. Fawcett JK, Scott JE (1960) A rapid and precise method for the determination of urea. *J Clin Pathol* 13(2):156–159. <https://doi.org/10.1136/jcp.13.2.156>
  34. Gochman N, Schmitz JM (1971) Automated determination of uric acid, with use of a uricase-peroxidase system. *Clin Chem* 17(12):1154–1159. <https://doi.org/10.1093/clinchem/17.12.1154>
  35. Jaffe MZ (1886) Über den Niedererhlag, welchen Pikrinsure in normalem Harn erzeugt und über eine neue Reaktion des Kreatinins. *Zschr Physiol Chem* 10:391–400. <https://doi.org/10.1515/bchm1.1886.10.5.391>
  36. Preuss HG, Jarrell ST, Scheckenbach R, Lieberman S, Anderson RA (1998) Comparative effect of chromium vanadium and Gymnema sylvestre on sugar-induced blood pressure elevation in SHR. *J Am Coll Nutr* 17(2):116–123. <https://doi.org/10.1080/07315724.1998.10718736>
  37. Marklund SL, Marklund G (1974) Involvement of the superoxide anion radical in the autoxidation of pyrogallol and a convenient assay for superoxide dismutase. *Eur J Biochem* 47(3):469–474. <https://doi.org/10.1111/j.1432-1033.1974.tb03714.x>
  38. Cohen G, Dembic D, Marcus J (1970) Measurement of catalase activity in tissue extract. *Anal Biochem* 34:30–38. [https://doi.org/10.1016/0003-2697\(70\)90083-7](https://doi.org/10.1016/0003-2697(70)90083-7)
  39. Kar M, Mishra D (1976) Catalase, Peroxidase and Polyphenoloxidase activities during rice leaf senescence. *Plant Physiol* 57(2):315–319. <https://doi.org/10.1104/pp.57.2.315>
  40. Beutler E, Duron O, Kelly BM (1963) Improved method for the determination of blood glutathione. *J Lab Clin Med* 61:882–888
  41. Livak KJ, Schmittgen TD (2001) Analysis of relative gene expression data using real-time quantitative PCR and the 2<sup>(-Delta Delta C(T))</sup> method. *Methods* 25(4):402–408. <https://doi.org/10.1006/meth.2001.1262>
  42. Bancroft J, Gamble M (2002) Theory and practice of histological techniques, 5th edn. Churchill Livingstone Pub, Edinburg, pp 172–175
  43. Kiernan JA (2001) Histological and histochemical methods: theory and practice, 3rd edn. Arnold Euston Road, London, pp 154–155
  44. MD Abrámoff PJ Magalhães S Ram 2004 Image processing with ImageJ *Biophotonics Int* 11 7 36 42
  45. Bozzola JJ, Russell LD (1999) Electron microscopy: principles and techniques for biologists, 2nd edn. Jones and Bartlett publishers, Boston, p 670
  46. Wu T, Ding L, Andoh V, Zhang J, Chen L (2023) The mechanism of hyperglycemia-induced renal cell injury in diabetic nephropathy disease: an update. *Life (Basel)* 13(2):539. <https://doi.org/10.3390/life13020539>
  47. Fraser DA, Hansen KF (2005) Making sense of advanced glycation end products and their relevance to diabetic complications. *Inter Diabetes Monitor* 17:1–7
  48. Han D, Yamamoto Y, Munesue S, Motoyoshi S, Saito H, Win MT, Watanabe T, Tsuneyama K, Yamamoto H (2013) Induction of receptor for advanced glycation end products by insufficient leptin action triggers pancreatic  $\beta$ -cell failure in type 2 diabetes. *Genes Cells* 18(4):302–314. <https://doi.org/10.1111/gtc.12036>
  49. Niu H, Li G, Qiao Y, Wang F (2019) Polydatin ameliorates renal fibrosis in a streptozotocin-induced rat model of diabetic nephropathy by inhibiting TLR4/NF- $\kappa\beta$  signaling. *Trop J Pharm Res* 18(11):2263–2269. <https://doi.org/10.4314/tjpr.v18i11.5>
  50. Dissanayake AM, Wheldon MC, Ahmed J, Hood CJ (2017) Extending metformin use in diabetic kidney disease: a pharmacokinetic study in stage 4 diabetic nephropathy. *Kidney Int Rep* 2(4):705–712. <https://doi.org/10.1016/j.ekir.2017.03.005>
  51. Ge X, Su Z, Wang Y, Zhao X, Hou K, Zheng S, Zeng P, Shi Z, Hu S, Wang Y, Zhou M, Zhang J, Li X (2023) Identifying the intervention mechanisms of polydatin in hyperuricemia model rats by using UHPLC-Q-Exactive Orbitrap mass spectroscopy metabolomic approach. *Front Nutr* 10:1117460. <https://doi.org/10.3389/fnut.2023.1117460>
  52. Abd El-Hameed AM (2020) Polydatin-loaded chitosan nanoparticles ameliorates early diabetic nephropathy by attenuating oxidative stress and inflammatory responses in streptozotocin-induced diabetic rat. *J Diabetes Metab Disord* 19(2):1599–1607. <https://doi.org/10.1007/s40200-020-00699-7>
  53. Yonekura H, Yamamoto Y, Sakurai S, Watanabe T, Yamamoto H (2005) Roles of the receptor for advanced glycation endproducts in diabetes-induced vascular injury. *J Pharmacol Sci* 97(3):305–311. <https://doi.org/10.1254/jphs.cpj04005x>
  54. Rahmani AH, Alsahli MA, Khan AA, Almatroodi SA (2023) Quercetin, a plant flavonol attenuates diabetic complications, renal tissue damage, renal oxidative stress and inflammation in streptozotocin-induced diabetic rats. *Metabolites* 13(1):130. <https://doi.org/10.3390/metabo13010130>
  55. Xu J, Liu LQ, Xu LL, Xing Y, Ye S (2020) Metformin alleviates renal injury in diabetic rats by inducing Sirt1/FoxO1 autophagic signal axis. *Clin Exp Pharmacol Physiol* 47(4):599–608. <https://doi.org/10.1111/1440-1681.13226>
  56. Zhang Z, Huang Q, Zhao D, Lian F, Li X, Qi W (2023) The impact of oxidative stress-induced mitochondrial dysfunction on diabetic microvascular complications. *Front Endocrinol (Lausanne)* 14:112363. <https://doi.org/10.3389/fendo.2023.1112363>
  57. Sheetz MJ, King GL (2002) Molecular understanding of hyperglycemia's adverse effects for diabetic complications. *JAMA* 288(20):2579–2588. <https://doi.org/10.1001/jama.288.20.2579>
  58. Zhang Q, Ames JM, Smith RD, Baynes JW, Metz TO (2009) A perspective on the Maillard reaction and the analysis of protein glycation by mass spectrometry: probing the pathogenesis of chronic disease. *J Proteome Res* 8(2):754–769. <https://doi.org/10.1021/pr800858h>
  59. Hayden MS, Ghosh S (2014) Regulation of NF- $\kappa\beta$  by TNF family cytokines. *Semin Immunol* 26(3):253–266. <https://doi.org/10.1016/j.smim.2014.05.004>
  60. Coto E, Díaz-Corte C, Tranche S, Gómez J, Alonso B, Iglesias S, Reguero JR, López-Larrea C, Coto-Segura P (2018) Gene variants in the NF- $\kappa\beta$  pathway (NFKB1, NFKBIA, NFKBIZ) and their association with type 2 diabetes and impaired renal function. *Hum Immunol* 79(6):494–498. <https://doi.org/10.1016/j.humimm.2018.03.008>
  61. Sun Y, Jin D, Zhang Z, Zhang Y, Zhang Y, Kang X, Jiang L, Tong X, Lian F (2023) Effects of antioxidants on diabetic kidney diseases: mechanistic interpretations and clinical assessment. *Chin Med* 18(1):3. <https://doi.org/10.1186/s13020-022-00700-w>
  62. Mathers J, Fraser JA, McMahon M, Saunders RD, Hayes JD, McLellan LI (2004) Antioxidant and cytoprotective responses to redox stress. *Biochem Soc Symp* 71:157–176. <https://doi.org/10.1042/bss0710157>
  63. Zhong W, Huan XD, Cao Q, Yang J (2015) Cardioprotective effect of epigallocatechin-3-gallate against myocardial infarction in hypercholesterolemic rats. *Exp Ther Med* 9(2):405–410. <https://doi.org/10.3892/etm.2014.2135>
  64. Satta S, Mahmoud AM, Wilkinson FL, Yvonne Alexander M, White SJ (2017) The role of Nrf2 in cardiovascular function and disease. *Oxid Med Cell Longev* 2017:9237263. <https://doi.org/10.1155/2017/9237263>
  65. Gold R, Kappos L, Arnold DL, Bar-Or A, Giovannoni G, Selmaj K, Tornatore C, Sweetser MT, Yang M, Sheikh SI, Dawson KT (2012) Placebo-controlled phase 3 study of oral bg-12 for relapsing multiple sclerosis. *N Engl J Med* 367(12):1098–1107. <https://doi.org/10.1056/NEJMoa1114287>
  66. Ganesh Yerra V, Negi G, Sharma SS, Kumar A (2013) Potential therapeutic effects of the simultaneous targeting of the Nrf2 and NF- $\kappa\beta$  pathways in diabetic neuropathy. *Redox Biol* 1(1):394–397. <https://doi.org/10.1016/j.redox.2013.07.005>
  67. Vijayalakshmi S, Mariadoss AVA, Ramachandran V, Shalini V, Agilan B, Sangeetha CC, Balu P, Kotakadi VS, Karthikkumar V, Ernest D (2019) Polydatin encapsulated poly [Lactic-co-glycolic acid] nanoformulation counteract the 7,12-dimethylbenz[a]anthracene mediated experimental carcinogenesis through the inhibition of cell proliferation. *Antioxidants* 8(9):375. <https://doi.org/10.3390/antiox8090375>
  68. Wang H, Zheng Z, Han W, Yuan Y, Li Y, Zhou K, Wang Q, Xie L, Xu K, Zhang H, Xu H, Wu Y, Xiao J (2020) Metformin promotes axon regeneration after spinal cord injury through inhibiting oxidative stress and stabilizing microtubule. *Oxid Med Cell Longev* 2020:9741369. <https://doi.org/10.1155/2020/9741369>
  69. Hassan FI, Didari T, Khan F, Niaz K, Mojtahedzadeh M, Abdollahi M (2020) A review on the protective effects of metformin in sepsis-induced organ failure. *Cell J* 21(4):363–370. <https://doi.org/10.22074/cellj.2020.6286>

70. Mohammad HMF, Galal Gouda S, Eladl MA, Elkazaz AY, Elbayoumi KS, Farag NE, Elshormilisy A, Al-Ammash BB, Hegazy A, Abdelkhalig SM, Mohamed AS, El-Dosoky M, Zaitone SA (2023) Metformin suppresses LRG1 and TGF $\beta$ 1/ALK1-induced angiogenesis and protects against ultrastructural changes in rat diabetic nephropathy. *Biomed Pharmacother* 158:114128. <https://doi.org/10.1016/j.biopha.2022.114128>
71. Hassan BN, Alazzouni AS, Fathalla AS (2023) Ameliorative effect of Metformin Nano emulsion against induced diabetic nephropathy in rat model: microanatomy study. *ABAS* 1(1):55–62. <https://doi.org/10.21608/ABAS.2023.195731.1010>
72. Tutun B, Elbe H, Vardi N, Parlakpınar H, Polat A, Gunaltılı M, Guclu MM, Yasar EN (2019) Dexpanthenol reduces diabetic nephropathy and renal oxidative stress in rats. *Biotech Histochem* 94(2):84–91. <https://doi.org/10.1080/10520295.2018.1508746>
73. Bheerreddy P, Yerra VG, Kalvala AK, Sherkhane B, Kumar A (2021) SIRT1 activation by polydatin alleviates oxidative damage and elevates mitochondrial biogenesis in experimental diabetic neuropathy. *Cell Mol Neurobiol* 41(7):1563–1577. <https://doi.org/10.1007/s10571-020-00923-1>
74. Li KX, Ji MJ, Sun HJ (2021) An updated pharmacological insight of resveratrol in the treatment of diabetic nephropathy. *Gene* 780:145532. <https://doi.org/10.1016/j.gene.2021.145532>
75. Chen ZQ, Sun XH, Li XJ, Xu ZC, Yang Y, Lin ZY, Xiao HM, Zhang M, Quan SJ, Huang HQ (2020) Polydatin attenuates renal fibrosis in diabetic mice through regulating the Cx32-Nox4 signaling pathway. *Acta Pharmacol Sin* 41(12):1587–1596. <https://doi.org/10.1038/s41401-020-0475-6>
76. Miko M, Jakubovsky J, Vrabcová M, Varga I (2016) Ultrastructural changes of kidney in diabetic rats. *Bratisl Med J* 117(3):161–165. [https://doi.org/10.4149/bll\\_2016\\_029](https://doi.org/10.4149/bll_2016_029)
77. Tyagi I, Agrawal U, Amitabh V, Jain AK, Saxena S (2008) Thickness of glomerular and tubular basement membranes in preclinical and clinical stages of diabetic nephropathy. *Indian J Nephrol* 18(2):64–69. <https://doi.org/10.4103/0971-4065.42336>
78. Ni Z, Tao L, Xiaohui Xu, Zelin Z, Jiangang L, Zhao S, Weikang H, Hongchao Xu, Qiuqing W, Xin LI (2017) Polydatin impairs mitochondria fitness and ameliorates podocyte injury by suppressing Drp1 expression. *J Cell Physiol* 232(10):2776–2787. <https://doi.org/10.1002/jcp.25943>

### Publisher's Note

Springer Nature remains neutral with regard to jurisdictional claims in published maps and institutional affiliations.

Submit your manuscript to a SpringerOpen<sup>®</sup> journal and benefit from:

- Convenient online submission
- Rigorous peer review
- Open access: articles freely available online
- High visibility within the field
- Retaining the copyright to your article

---

Submit your next manuscript at ► [springeropen.com](https://www.springeropen.com)

---